Turkish Journal of Chemistry

Volume 47 | Number 6 Article 5

12-29-2023

Phytochemical investigation on the aerial parts of Veratrum versicolor f. viride Nakai and their biological activities

SEONG SU HONG
bestgene@gbsa.or.kr

JAE YEON LEE
jyeon@gbsa.or.kr

YEON WOO JEONG
jion123@gbsa.or.kr

JI EUN LEE
jieun@gbsa.or.kr

YUN-HYEOK CHOI
choiyh1400@gbsa.or.kr

See next page for additional authors

Phytochemical investigation on the aerial parts of Veratrum versicolor f. viride Nakai and their biological activities

Authors

SEONG SU HONG, JAE YEON LEE, YEON WOO JEONG, JI EUN LEE, YUN-HYEOK CHOI, WONSIK JEONG, Eun-Kyung AHN, CHUN WHAN CHOI, IL HO AHN, and JOA SUB OH

TÜBİTAK

Turkish Journal of Chemistry

http://journals.tubitak.gov.tr/chem/

Research Article

Turk J Chem
(2023) 47: 1346-1354
© TÜBİTAK
doi:10.55730/1300-0527.3618

Phytochemical investigation on the aerial parts of *Veratrum versicolor* f. *viride* Nakai and their biological activities

Seong Su HONG[1,†*], Jae Yeon LEE[1,†], Yeon Woo JEONG[1], Ji Eun LEE[1], Yun-Hyeok CHOI[1], Wonsik JEONG[1], Eun-Kyung AHN[1], Chun Whan CHOI[1], Il Ho AHN[2], Joa Sub OH[3]

[1]Bio-Center, Gyeonggido Business & Science Accelerator (GBSA), Suwon, Republic of Korea
[2]NewCellPharm Co., Ltd., Seongnam, Republic of Korea
[3]College of Pharmacy, Dankook University, Cheonan, Republic of Korea

Received: 08.02.2023 • **Accepted/Published Online:** 12.09.2023 • **Final Version:** 29.12.2023

Abstract: *Veratrum* spp. have traditionally been used in folk medicine to treat various pathologies. In this study, nine compounds, comprising one simple phenolic compound (**1**), three stilbenoids (**2**–**4**), and five flavonoids (**5**–**9**), were isolated from the aerial parts of *Veratrum versicolor* f. *viride* Nakai. The structures of these compounds were elucidated by spectroscopic analyses and comparison with reported data. Together, all reported compounds were isolated from *V. versicolor* f. *viride* for the first time in the study. Among them, two flavone aglycone tricetins (**7** and **9**) have never been isolated from the genus *Veratrum* or the family Melanthiaceae. The ethanol extract and isolated compounds were assessed for their inhibitory effects on elastase, tyrosinase, and melanin synthesis. Compounds **5** and **7** inhibited elastase (IC_{50}: 292.25 ± 14.39 and 800.41 ± 5.86 μM, respectively), whereas compounds **2**–**5** inhibited tyrosinase with IC_{50} values in the range of 6.42 ~ 51.19 μM, respectively. In addition, compounds **3**–**6** and **8** exhibited dose-dependent inhibition (70.4% ~ 91.0%) of melanogenesis at a concentration of 100 μM.

Key words: *Veratrum*, flavonoid, stilbenoid, tyrosinase, elastase, melanogenesis

1. Introduction

The genus *Veratrum* is a member of the family Melanthiaceae and consists of approximately 40 plant species distributed in temperate regions of the Northern Hemisphere, including Asia, Europe, and North America [1]. There are seven species (*V. coreanum* O.Loes., *V. dahuricum* O.Loes., *V. dolichopetalum* O.Loes., *V. maackii* Regel., *V. nigrum* L., *V. oxysepalum* Turcz., and *V. versicolor* Nakai), three varieties (*V. bohnhofii* var. *latifolium* Nakai, *V. maackii* var. *japonicum* (Baker) T.Shimizu, and *V. maackii* var. *parviflorum* (Maxim. ex Miq.) H.Hara), and two forms (*V. versicolor* f. *brunnea* Nakai and *V. versicolor* f. *viride* Nakai) in Korea that are widely spread across the Korean peninsula [2]. The rhizomes and roots of *V. nigrum* and *V. oxysepalum* have been used in traditional Korean medicine for centuries and are denoted as "Veratri Rhizoma et Radix" in the Korean Herbal Pharmacopoeia. These plants are indicated for the treatment of inflamed tonsils, snakebites, sore throats, coughs, dyspnea in epilepsy or stroke patients, and wrist pain [3]. Several species of *Veratrum* (*V. album* L., *V. californicum* Durand, *V. viride* Röhl., and *V. nigrum* var. *japonicum* (Baker) T.Shimizu) are harmful to humans and animals, and earlier research has shown that steroidal alkaloid constituents are responsible for this toxicity [4]. *Veratrum* species are rich sources of plant-derived steroidal alkaloids [5,6]. Among the various types of steroidal alkaloids, veratrum-type steroidal alkaloids, which are the most frequently found in the genus *Veratrum*, can be categorized into five subtypes: cevanine, veratramine, jervine, solanidine, and verazine [6]. Moreover, many of these *Veratrum* alkaloids have been reported to possess a range of biological activities, such as antiproliferative [5], antidiabetic [7], anticancer [8], antifungal [9], antihypertensive [10], antiinflammatory [11], antioxidant [12], and potent analgesic [13,14] properties. Previous phytochemical investigations of the chemical constituent species in *Veratrum* have identified a diverse range of compounds, including arylbenzofurans [15], cevanine-type alkaloids [16], veratramine-type alkaloids [14], jervine-type alkaloids [12,17], solanidine-type alkaloids [18], verazine-type alkaloids [19], flavonoids [20], stilbene glycosides [21], and aurones [22]. To date, most studies on *Veratrum* spp. have focused on steroidal alkaloids. However, to the best of our knowledge, no previous investigations have been conducted on the phytochemical and pharmacological properties of the constituents of *V. versicolor* f. *viride*.

* Correspondence: bestgene@gbsa.or.kr
† These authors contributed equally to this work.

2. Materials and methods

2.1. General

Nuclear magnetic resonance (NMR) spectra were recorded on a Bruker Ascend III 700 spectrometer (Bruker BioSpin GmbH., Rheinstetten, Germany) in DMSO-d_6 and CD_3OD at room temperature. Chemical shifts are in ppm (δ), relative to tetramethylsilane as an internal standard, and coupling constants are in hertz; ^1H, ^{13}C, DEPT, COSY, HSQC, and HMBC were performed using the standard pulse sequences. Electrospray ionization mass (ESI-MS) spectra were acquired on an Agilent 6130 series quadrupole LC/MS System (Agilent Technologies, Santa Clara, CA, USA). Open column chromatography was performed using Diaion HP-20 adsorbent resin (Mitsubishi Chemical Corp, Tokyo, Japan). Medium-pressure liquid chromatography (MPLC) was conducted using a CombiFlash Rf flash chromatography system (Teledyne ISCO Inc., Lincoln, NE, USA), and the separations were performed on a Redi*Sep*® Rf C_{18} column with a flow rate of 40 mL/min. Preparative high-performance liquid chromatography (HPLC) was performed on a Thermo Scientifc Dionex Ultimate 3000 UHPLC system (Thermo Fisher Scientific Inc., Waltham, MA, USA) equipped with an HPG-3200BX biocompatible binary semipreparative pump and a rapid separations PDA detector (Ultimate DAD-3000) controlled by Chromeleon 7.2 software. The separations were carried out on a Kromasil 100-5-C18 column (5 μm, 21.2 × 250 mm, Nouryon Chemicals Finance B.V., Amsterdam, Netherlands). Thin layer chromatography (TLC) was performed using DC-Fertigfolien ALUGRAM SIL G/$UV_{254+366}$ (0.2 mm, Macherey-Nagel GmbH & Co. KG, Düren, Germany) plates, and spots were visualized by a 10% vanillin–sulfuric acid reagent. All chemicals and solvents were of analytical grade and were used without further purification.

2.2. Plant material

The aerial parts of *V. versicolor* f. *viride* Nakai [23] were collected from Cheorwon-gun, Gangwon-do, Republic of Korea, in July 2022. The collection area is 868 m above sea level and located at GPS 38°8′30.87″N 127°26′22.95″E and they grow naturally at the edge of the ridge. Organic matter in soil is moderate (2%∼4%) and it is black forest soil. The crown density is 80% and the quantity of light is poor. The botanical materials were authenticated by one of the authors (Prof. J.S. Oh) and a voucher specimen (G105) was deposited at the Bio-Center, Gyeonggido Business & Science Accelerator (GBSA), Suwon, Republic of Korea.

2.3. Extraction and isolation

The shade-dried aerial parts of *V. versicolor* f. *viride* (2 kg) were percolated with 70% aqueous EtOH at room temperature. Following evaporation of the solvent under reduced pressure, the residue (265 g) was suspended in water and successively partitioned with CH_2Cl_2, EtOAc, and water-saturated *n*-BuOH to yield the respective extracts (17 g, 12.5 g, and 24 g) after being concentrated to dryness. The crude extracts and solvent layers of *V. versicolor* f. *viride* were screened for their inhibitory effects on tyrosinase, elastase, and melanogenesis at various concentrations (5 ~ 1000 μg/mL) (Figure 1). The results showed that the EtOAc layer exhibited dose-dependent inhibitory activity. Part of the EtOAc-soluble fraction was chromatographed over a Diaion HP-20 resin and eluted with a water–MeOH stepwise gradient solvent system (1:0 to 0:1) to yield five fractions ($G105B_1$–$G105B_5$). Fraction $G105B_3$ (1.5 g) was subjected to MPLC over an ODS column (RediSep Rf silica gold 150 g, 40 mL/min, 120 min) by eluting with a gradient mixture of 10% ~ 35% acetonitrile in water to yield compounds 1 (16.2 mg, t_R = 25.2 min), **2** (45.3 mg, t_R = 41.1 min), 3 (96.4 mg, t_R = 47.4 min), and 4 (73.1 mg, t_R = 71.4 min). Subfraction $G105B_4$ (86.9 mg) was subjected to the above MPLC system (acetonitrile–H_2O, 20:80 to 40:60, v/v), resulting in the isolation of compounds **5** (36.6 mg, t_R = 37.8 min) and 9 (1.3 mg, t_R = 42.8 min). Compound 6 (15.1 mg, t_R = 78.1 min) and two compound mixtures ($G105C_4$, 15.1 mg, t_R = 81.5 min) were isolated from subfraction $G105B_5$ using MPLC (acetonitrile–water, 15:85 to 45:55 in 120 min). Further purification of subfraction $G105C_4$ was performed using preparative HPLC (Kromasil 100-5-C18 column; 21.2 × 250 mm; flow rate, 10 mL/min; solvent A, 0.05% TFA in water; solvent B, acetonitrile; gradient elution 0 min 30% B to 120 min 40% B, detection at 210 and 350 nm). HPLC separation led to purification of compounds 7 (36.2 mg, t_R = 38.2 min) and 8 (11.2 mg, t_R = 41.8 min). The isolation process used in the present study is summarized in Figure S1 (Supporting Information).

2.4. Spectral data of isolated compounds

The structures of the isolated compounds were elucidated by MS and 1D/2D NMR data analyses and compared with the corresponding data reported in the literature.

Vanillic acid (1): White amorphous powder, ^1H NMR (CD_3OD, 700 MHz): δ 7.56 (1H, dd, *J* = 8.4, 2.1 Hz, H-6), 7.56 (1H, d, *J* = 2.1 Hz, H-2), 6.84 (1H, d, *J* = 8.4 Hz, H-5), 3.89 (3H, s, 3-O$\underline{CH}_3$); ^{13}C NMR (CD_3OD, 175 MHz): δ 170.2 (C-7), 152.8 (C-4), 148.8 (C-3), 123.3 (C-1), 125.4 (C-6), 116.0 (C-5), 113.9 (C-2), 56.4 (3-O$\underline{C}H_3$); UV (CH_3OH) λ_{max} nm: 204, 218, 260, 291; ESIMS (positive ion mode) *m/z* 169 $[M + H]^+$; (Supporting Information, Figures S2 and S3) [24].

***trans*-Piceid (2):** Pale brown amorphous powder, ^1H NMR (CD_3OD, 700 MHz): δ 7.36 (2H, d, *J* = 9.1 Hz, H-2′, 6′), 7.02 (1H, d, *J* = 16.1 Hz, H-8), 6.85 (1H, d, *J* = 16.1 Hz, H-7), 6.76 (2H, d, *J* = 9.1 Hz, H-3′, 5′), 6.79 (1H, t, *J* = 2.1 Hz, H-2), 6.61

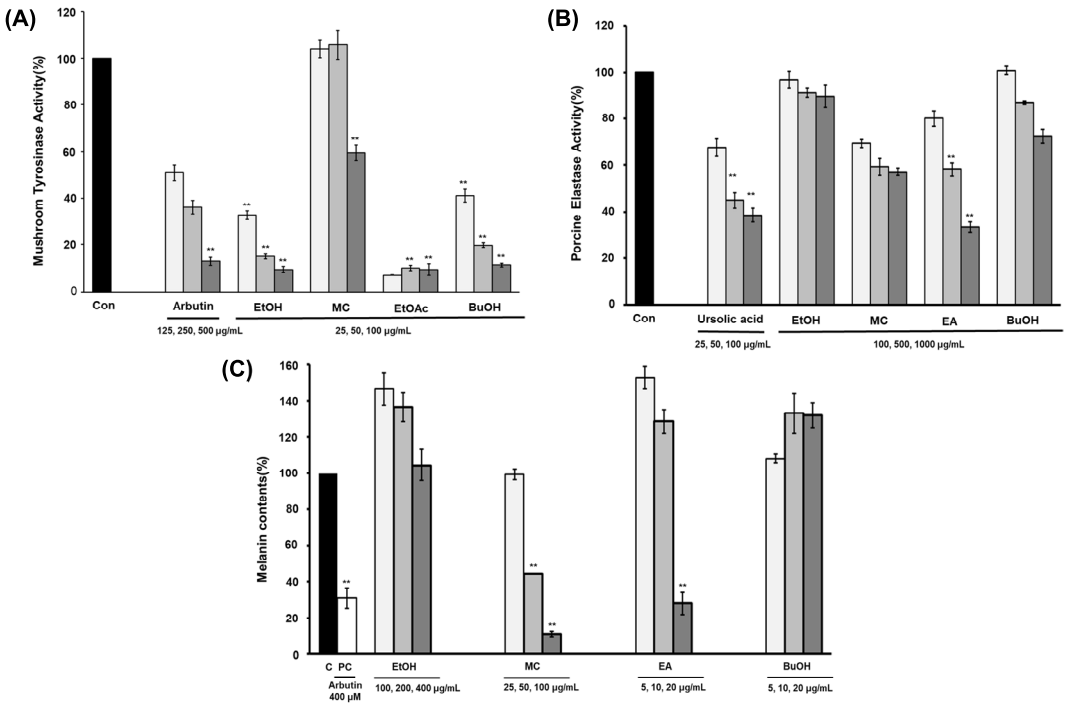

Figure 1. Tyrosinase (A), elastase (B), and melanogenesis (C) inhibitory activity of extracts obtained from aerial parts of *V. versicolor* f. *viride*. The asterisks represent a significant difference between the columns. **, $p < 0.01$. The bars represent standard errors.

(1H, t, *J* = 2.1 Hz, H-6), 6.45 (1H, t, *J* = 2.1 Hz, H-4), 4.89 (1H, d, *J* = 7.7 Hz, H-1″), 3.93 (1H, dd, *J* = 11.9, 2.1 Hz, H_a-6″), 3.71 (1H, dd, *J* = 11.9, 5.6 Hz, H_b-6″), 3.47 (1H, t, *J* = 9.1 Hz, H-5″), 3.46 (1H, m, H-3″), 3.45 (1H, t, *J* = 9.1 Hz, H-2″), 3.38 (1H, t, *J* = 9.1 Hz, H-4″); ^{13}C NMR (CD_3OD, 175 MHz): δ 160.6 (C-3), 159.7 (C-5), 158.6 (C-4′), 141.6 (C-1), 130.5 (C-1′), 130.1 (C-8), 129.1 (C-2′, 6′), 126.8 (C-7), 116.2 (C-3′, 5′), 108.5 (C-6), 107.1 (C-2), 104.2 (C-4), 102.5 (C-1″), 78.4 (C-5″), 78.2 (C-3″), 75.1 (C-2″), 71.6 (C-4″), 62.7 (C-6″); UV (CH_3OH) λ_{max} nm: 214, 233 (sh), 306, 319; ESIMS (positive ion mode) *m/z* 391 $[M + H]^+$; (Supporting Information, Figures S4 and S5) [25].

Oxyresveratrol (3): Pale brown amorphous powder, ^{1}H NMR (CD_3OD, 700 MHz): δ 7.32 (1H, d, *J* = 8.4 Hz, H-6′), 7.26 (1H, d, *J* = 16.1 Hz, H-8), 6.81 (1H, d, *J* = 16.1 Hz, H-7), 6.44 (2H, d, *J* = 2.1 Hz, H-2, 6), 6.30 (1H, dd, *J* = 8.4, 2.1 Hz, H-5′), 6.29 (1H, d, *J* = 2.1 Hz, H-3′), 6.13 (1H, t, *J* = 2.1 Hz, H-4); ^{13}C NMR (CD_3OD, 175 MHz): δ 159.6 (C-3, 5), 159.4 (C-4′), 157.5 (C-2′), 142.2 (C-1), 118.0 (C-1′), 124.9 (C-8), 128.5 (C-6′), 126.6 (C-7), 108.5 (C-5′), 103.7 (C-3′), 105.8 (C-2, 6), 102.4 (C-4); UV (CH_3OH) λ_{max} nm: 217, 239 (sh), 301, 327; ESIMS (positive ion mode) *m/z* 245 $[M + H]^+$; (Supporting Information, Figures S6 and S7) [26].

Resveratrol (4): Pale brown amorphous powder, ^{1}H NMR (CD_3OD, 700 MHz): δ 7.35 (2H, d, *J* = 8.4 Hz, H-2′, 6′), 6.95 (1H, d, *J* = 16.1 Hz, H-8), 6.80 (1H, d, *J* = 16.1 Hz, H-7), 6.76 (2H, d, *J* = 8.4 Hz, H-3′, 5′), 6.45 (2H, d, *J* = 2.1 Hz, H-2, 6), 6.16 (1H, t, *J* = 2.1 Hz, H-4); ^{13}C NMR (CD_3OD, 175 MHz): δ 159.7 (C-3, 5), 158.5 (C-4′), 141.3 (C-1), 130.6 (C-1′), 129.5 (C-8), 128.9 (C-2′, 6′), 127.1 (C-7), 116.6 (C-3′, 5′), 105.9 (C-2, 6), 102.8 (C-4); UV (CH_3OH) λ_{max} nm: 216, 237 (sh), 304, 319; ESIMS (positive ion mode) *m/z* 229 $[M + H]^+$; (Supporting Information, Figures S8 and S9) [27].

Luteolin (5): Yellow amorphous powder, ^{1}H NMR (DMSO-d_6, 700 MHz): δ 12.99 (1H, s, 5-OH), 10.83 (1H, s, 7-OH), 9.93 (1H, s, 4′-OH), 9.41 (1H, s, 3′-OH), 7.42 (1H, dd, *J* = 8.4, 2.1 Hz, H-6′), 7.40 (1H, d, *J* = 2.1 Hz, H-2′), 6.90 (1H, d, *J* = 8.4 Hz, H-5′), 6.78 (1H, s, H-3), 6.45 (1H, d, *J* = 2.1 Hz, H-8), 6.20 (1H, d, *J* = 2.1 Hz, H-6); ^{13}C NMR (DMSO-d_6, 175 MHz): δ 181.7 (C-4), 164.1 (C-7), 163.9 (C-2), 161.5 (C-5), 157.3 (C-9), 149.7 (C-4′), 145.7 (C-3′), 121.5 (C-1′), 119.0 (C-6′), 116.0 (C-5′), 113.4 (C-2′), 103.7 (C-10), 102.9 (C-3), 98.8 (C-6), 93.8 (C-8); UV (CH_3OH) λ_{max} nm: 206, 252, 269, 347; ESIMS (positive ion mode) *m/z* 289 $[M + H]^+$; (Supporting Information, Figures S10 and S11) [28].

Apigenin (6): Yellow amorphous powder, ^{1}H NMR (DMSO-d_6, 700 MHz): δ 12.97 (1H, s, 5-OH), 10.85 (1H, s, 7-OH), 10.37 (1H, s, 4′-OH), 7.93 (2H, d, *J* = 8.4 Hz, H-2′, 6′), 6.93 (2H, d, *J* = 8.4 Hz, H-3′, 5′), 6.79 (1H, s, H-3), 6.49 (1H, d, *J* = 2.1 Hz, H-8), 6.20 (1H, d, *J* = 2.1 Hz, H-6); ^{13}C NMR (DMSO-d_6, 175 MHz): δ 181.8 (C-4), 164.1 (C-7), 163.7 (C-2),

161.5 (C-5), 161.2 (C-4′), 157.3 (C-9), 128.5 (C-2′, 6′), 121.2 (C-1′), 116.0 (C-3′, 5′), 103.7 (C-10), 102.8 (C-3), 98.8 (C-6), 94.0 (C-8); UV (CH_3OH) λ_{max} nm: 207, 266, 337; ESIMS (positive ion mode) *m/z* 271 $[M + H]^+$; (Supporting Information, Figures S12 and S13) [28].

Tricin (7): Yellow amorphous powder, ^{1}H NMR (DMSO-d_6, 700 MHz): δ 12.97 (1H, s, 5-OH), 10.81 (1H, s, 7-OH), 9.34 (1H, s, 4′-OH), 7.32 (2H, s, H-2′, 6′), 6.98 (1H, s, H-3), 6.56 (1H, d, *J* = 2.1 Hz, H-8), 6.20 (1H, d, *J* = 2.1 Hz, H-6), 3.88 (6H, s, 3′, 5′-OC$\underline{H}_3$); ^{13}C NMR (DMSO-d_6, 175 MHz): δ 181.8 (C-4), 164.1 (C-7), 163.7 (C-2), 161.4 (C-5), 157.3 (C-9), 148.2 (C-3′, 5′), 139.8 (C-4′), 120.4 (C-1′), 104.3 (C-2′, 6′), 103.7 (C-10), 103.6 (C-3), 98.8 (C-6), 94.2 (C-8), 56.4 (3′,5′-O$\underline{C}H_3$); UV (CH_3OH) λ_{max} nm: 209, 243 (sh), 270, 351; ESIMS (positive ion mode) *m/z* 331 $[M + H]^+$; (Supporting Information, Figures S14 and S15) [29].

Chrysoeriol (8): Yellow amorphous powder, ^{1}H NMR (DMSO-d_6, 700 MHz): δ 12.98 (1H, s, 5-OH), 10.86 (1H, s, 7-OH), 9.99 (1H, s, 4′-OH), 7.57 (1H, dd, *J* = 8.4, 2.1 Hz, H-6′), 7.56 (1H, d, *J* = 2.1 Hz, H-2′), 6.91 (1H, s, H-3), 6.84 (1H, d, *J* = 8.4 Hz, H-5′), 6.52 (1H, d, *J* = 2.1 Hz, H-8), 6.20 (1H, d, *J* = 2.1 Hz, H-6), 3.90 (3H, s, 3′-OC$\underline{H}_3$); ^{13}C NMR (DMSO-d_6, 175 MHz): δ 181.8 (C-4), 164.1 (C-7), 163.7 (C-2), 161.4 (C-5), 157.3 (C-9), 150.7 (C-4′), 148.0 (C-3′), 121.5 (C-1′), 120.4 (C-6′), 115.8 (C-5′), 110.2 (C-2′), 103.7 (C-10), 103.2 (C-3), 98.8 (C-6), 94.1 (C-8), 56.0 (3′-O$\underline{C}H_3$); UV (CH_3OH) λ_{max} nm: 206, 250, 266, 346; ESIMS (positive ion mode) *m/z* 301 $[M + H]^+$; (Supporting Information, Figures S16 and S17) [30].

3′-*O*-Methyltricetin (9): Yellow amorphous powder, ^{1}H NMR (DMSO-d_6, 700 MHz): δ 13.09 (1H, s, 5-OH), 10.79 (1H, s, 7-OH), 9.42 (1H, s, 5′-OH), 9.25 (1H, s, 4′-OH), 7.17 (1H, d, *J* = 2.1 Hz, H-2′), 7.15 (1H, d, *J* = 2.1 Hz, H-6′), 6.83 (1H, s, H-3), 6.47 (1H, d, *J* = 2.1 Hz, H-8), 6.20 (1H, d, *J* = 2.1 Hz, H-6), 3.88 (3H, s, 3′-OC$\underline{H}_3$); ^{13}C NMR (DMSO-d_6, 175 MHz): δ 181.7 (C-4), 164.0 (C-7), 163.9 (C-2), 161.4 (C-5), 157.3 (C-9), 148.6 (C-3'), 145.9 (C-5′), 138.6 (C-4′), 120.4 (C-1′), 107.5 (C-6′), 103.7 (C-10), 103.3 (C-3), 102.4 (C-2′), 98.8 (C-6), 93.9 (C-8), 56.2 (3′-O$\underline{C}H_3$); UV (CH_3OH) λ_{max} nm: 209, 266, 352; ESIMS (positive ion mode) *m/z* 317 $[M + H]^+$; (Supporting Information, Figures S18 and S19) [31].

2.5. Biological assay

2.5.1. Tyrosinase inhibition assay

The reaction was carried out in a 0.1 M potassium phosphate buffer (pH 6.5) containing 1.5 mM L-tyrosine and 1250 unit/mL mushroom tyrosinase and the reaction mixture was incubated at 37 °C for 20 min. The test samples were assayed for tyrosinase inhibition by measuring its effect on tyrosinase activity using an ELISA reader at 490 nm. Arbutin was used as a positive control. The inhibitory activity of the sample was expressed as the concentration that inhibits 50% of the enzyme activity (IC_{50}) [32].

2.5.2. Elastase inhibition assay

The reaction was carried out in a 50 mM Tris-HCl buffer (pH 8.5) containing 1 mg/mL N-succinyl-(Ala)3-p-nitroanilide and 0.6 U/mL PPE (porcine pancreas elastase). The test sample was added to the reaction mixture, and elastase inhibition was incubated at 25 °C for 10 min. The change in absorbance was measured at 405 nm using an ELISA reader. Ursolic acid was used as a positive control. The inhibitory activity of the sample was expressed as the concentration that inhibits 50% of the enzyme activity (IC_{50}) [33,34].

2.5.3. Cell culture

B16F10 mouse melanoma cells were cultured in DMEM medium containing 10% FBS and 1% penicillin-streptomycin in a 37 °C incubator with 5% CO_2. The cells were seeded in 100-mm tissue culture dishes to be used for subsequent experiments [32].

2.5.4. Measurement of relative melanin contents

B16F10 cells (1×10^5/well) were seeded in 6 well plates for 24 h. The cells were then incubated in the presence of 100 nM α-MSH, and treated with various concentrations (25, 50, and 100 μM) of sample for 72 h. After being washed twice with PBS, the cells were dissolved of 1 N NaOH and 10% DMSO, incubated at 60 °C for 1 h, and mixed to solubilize the melanin. Relative melanin content was determined with an ELISA reader by absorbance at 405 nm [32].

2.5.5. Statistical analysis

All data are presented as means ± standard deviation (SD). The results were analyzed for statistical significance using Student's t-test and one-way analysis of variance (ANOVA). Values of $^*p < 0.05$ and $^{**}p < 0.01$ were considered statistically significant.

3. Results and discussion

In the present study, nine compounds were isolated from the aerial parts of *V. versicolor* f. *viride*, comprising one phenolic analog (1), three stilbenoids (2–4), and five flavonoids (5–9) (Figure 2). The compounds isolated were identified as vanillic acid (1), *trans*-piceid (2), oxyresveratrol (3), resveratrol (4), luteolin (5), apigenin (6), and chrysoeriol (8) by comparing their spectroscopic data with reference values from previously published literature (Figure 2).

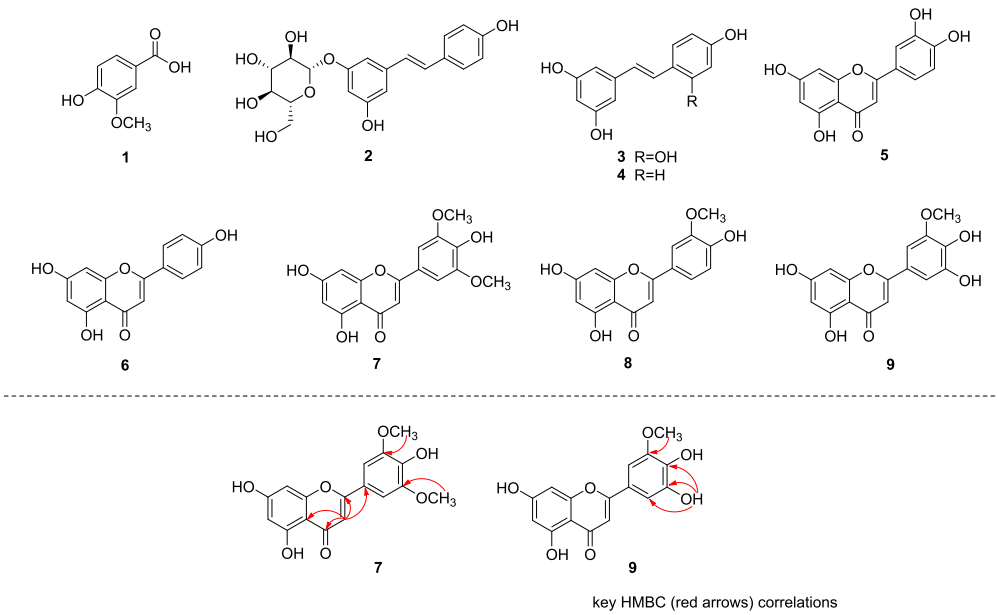

Figure 2. Chemical structures of compounds **1**–**9** identified from *V. versicolor* f. *viride*.

Compound 7 was obtained as a pale yellow amorphous powder. The UV spectrum showed maximum absorption bands of a flavonoid system at λ_{max} 351, 270, and 209 nm. The ^{1}H NMR data showed the presence of two *meta*-coupled aromatic protons [δ_H 6.56 1H, d, J = 2.1 Hz, H-8), 6.20 (1H, d, J = 2.1 Hz, H-6)], a symmetrical 1,3,4,5-tetrasubstitution of the benzene ring [δ_H 7.32 (2H, s, H-2′, H-6′)], one isolated aromatic proton [δ_H 6.98 (1H, s, H-3)], and two methoxyls [δ_H 3.88 (6H, s)]. Combined with the ^{13}C NMR, the DEPT and HSQC spectra of **7** exhibited resonances for 17 signals, including one conjugated carbonyl carbon (δ_C 181.8), seven oxygenated sp^2 carbons (δ_C 164.1, 163.7, 161.4, 157.3, 148.2 × 2, and 139.8), two quaternary carbons (δ_C 120.4 and 103.7), five aromatic methine carbons (δ_C 104.3 × 2, 103.6, 98.8, and 94.2), and two methoxy groups (δ_C 56.4 × 2). A comparison of the NMR data of 7 with those of tricetin (flavonoid) [35] revealed the presence of an additional methoxy group, suggesting that 7 was the methylated derivative of tricetin. The HMBC experiment of 7 showed correlations between methoxy signal (δ_H 3.88)/C-3′ and C-5′ (δ_C 148.2), confirming the substitution of the methoxyl group at C-3′ and C-5′ (Figure 2). Consequently, the structure of **7** was established to be 4′,5,7-trihydroxy-3′,5′-dimethoxyflavone (tricin) [29].

The structure of 9 was closely related to 7 based on UV and ^{1}H and ^{13}C NMR spectroscopic data. However, 9 had one carbon and two protons less than **7**. The appearance of a sharp singlet at δ_H 9.42 in the ^{1}H NMR spectrum of 9 and the absence of the signals of a methoxy group and a methoxy carbon in the ^{1}H and ^{13}C NMR spectra of 9, respectively, suggested a hydrogen bonded phenolic hydroxyl group at C-5′. The HMBC experiment of 9 showed correlations between 5′-OH (δ_H 9.42)/C-5′ (δ_C 145.9), C-4′ (δ_C 138.6) and C-6′ (δ_C 107.5), confirming the substitution of the phenolic hydroxyl group at C-5′ (Figure 2). On the basis of this evidence, the structure of the molecule was confirmed as 4′,5′,5,7-tetrahydroxy-3′ methoxyflavone (3′-*O*-methyltricetin) [31]. To the best of our knowledge, this is the first report of all aforementioned compounds being isolated from this plant, as well as compounds 7 and 9 from the family Melanthiaceae. The HPLC profiles of the isolated compounds are shown in Figure 3.

The tyrosinase inhibitory effects of the isolated compounds were examined, and IC_{50} was calculated using a dose-dependent response curve. The IC_{50} values for compounds 2–5 were as follows: 51.19 ± 5.50, 6.42 ± 0.45, 19.82 ± 0.77, and 37.89 ± 1.04 μM, respectively (Table). The IC_{50} values of arbutin (tyrosinase inhibitor) as a positive control were 473.65 μM [36]. With this bioassay, no tyrosinase inhibitory activity (IC_{50} > 100 M) was detected for other compounds. Moreover, inhibition of elastase enzyme (porcine pancreas) activity was used to evaluate the antiaging properties of the isolated compounds, and the results are shown in the Table. It was observed that compounds 5 and 8 showed moderate antielastase activity with IC_{50} values of 292.25 ± 14.39 and 800.41 ± 5.86 μM, respectively, compared to ursolic acid [37] (IC_{50}: 96.88 μM), which was used as the positive control. A melanin content assay was conducted to observe the inhibitory effect of the isolated constituents on melanin production. Here B16F10 melanoma cells were stimulated by α-MSH and cotreated with

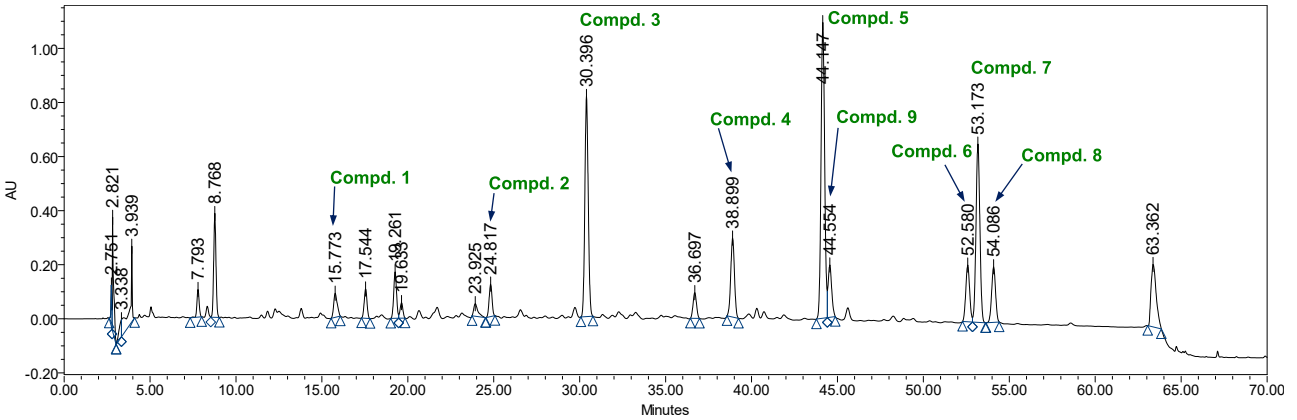

Figure 3. HPLC–PDA chromatographic profile of the EtOAc-soluble extract from *Veratrum versicolor* f. *viride* aerial parts was recorded at 210 nm. Column, YMC-Triart C18 (250 × 4.6 mm I.D., 5 μm); mobile phase, 0.05% trifluoroacetic acid in water (A) and acetonitrile (B), initial 90:10 (A:B, v/v), 60 min 60:40 (A:B, v/v); flow rate, 1 mL/min.

Table. In vitro tyrosinase and elastase inhibitory activity of the isolated compounds.

Compound	Tyrosinase inhibitory activity	Elastase inhibitory activity
	IC_{50} [a] (μM)	
1	>100	>1000
2	51.19 ± 5.50	>1000
3	6.42 ± 0.45	>1000
4	19.82 ± 0.77	>1000
5	37.89 ± 1.04	292.25 ± 14.39
6	>100	>1000
7	>100	>1000
8	>100	800.41 ± 5.86
Arbutin[b]	473.65 ± 18.21	-
Ursolic acid[b]	-	96.88 ± 1.33
[a]All compounds were examined in a set of experiments three times. [b]Positive control.		

compounds in three different concentrations (25, 50, and 100 μM) or arbutin (400 μM). According to the results shown in Figure 4, compounds 4, 5, and 8 greatly decreased the melanin content in α-MSH-stimulated B16F10 melanoma cells at 100 μM, as compared to those of arbutin. In the range of 50 ~ 100 μM, the inhibition percentages of resveratrol (4), luteolin (**5**), and chrysoeriol (8) were 72.7% ~ 82.7%, 83.5% ~ 91.0%, and 72.6% ~ 76.6%, respectively, whereas the inhibition rate of 400 μM arbutin was 69.2% (Supporting Information, Table S1) [38]. In conclusion, extracts and active compounds effectively inhibited elastase and mushroom tyrosinase activities and inhibited melanin synthesis by B16F10 melanoma cells. Thus, *V. versicolor* f. *viride* extracts and several of their chemical constituents can be considered useful for application in developing multitarget cosmeceuticals.

4. Conclusion

As part of our ongoing work in the search for biologically active constituents from Korean resource plants, an EtOH extract of *V. versicolor* f. *viride* was selected for phytochemical investigation. Nine natural compounds were isolated from the aerial parts of *V. versicolor* f. *viride*, comprising one phenolic analog (1), three stilbenoids (2–4), and five flavonoids (5–9), and the effectiveness of their biological potential was demonstrated. Based on enzyme and cell inhibitory assays, the

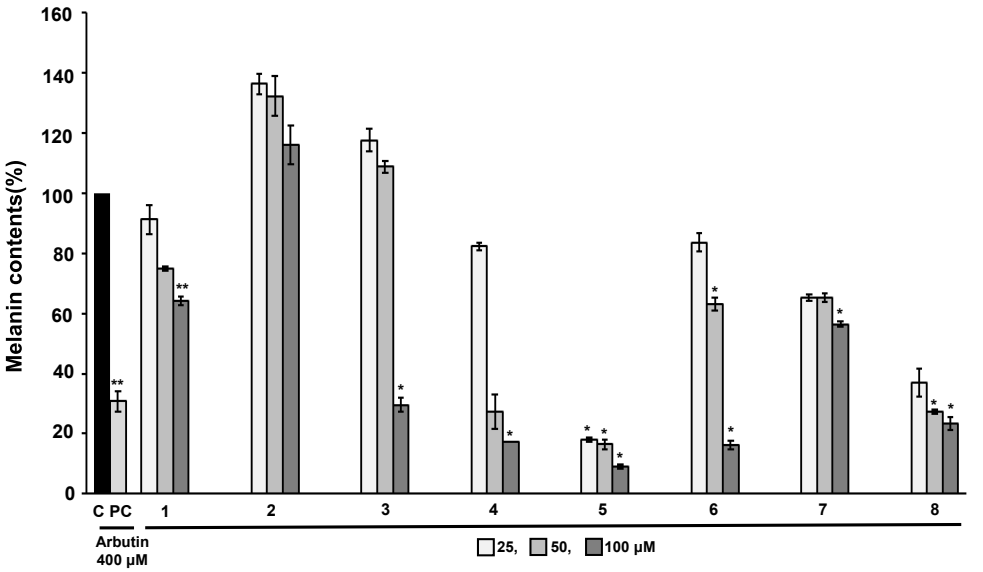

Figure 4. Effects of isolated compounds and arbutin (positive control) on melanin production in B16F10 mouse melanoma cells. The data are expressed as the mean value ± standard deviation of three independent experiments (*, $p < 0.05$).

isolated compounds could exhibit good antityrosinase, antielastase properties, and melanogenesis in B16F10 melanoma cells, thereby conferring a comprehensive attenuating effect against skin aging-related factors. Hence, the results of our study suggest that *V. versicolor* f. *viride* has great potential to be used as an effective multifunctional bioactive agent for cosmeceutical formulations. However, additional in-depth studies and clinical evaluations are needed to estimate the skincare potential of extracts and active compounds.

Acknowledgments
This study was carried out with the support of the R&D Program for Forest Science Technology (Project No. 2022441A00-2222-0103) provided by the Korea Forest Service (Korea Forestry Promotion Institute). We would like to thank Editage (www.editage.co.kr) for English language editing.

Conflict of interest
The authors declare no conflict of interest.

References

[1] Dirks ML, Seale JT, Collins JM, McDougal OM. Review: *Veratrum californicum* alkaloids. Molecules 2021; 26 (19): 5934. https://doi.org/10.3390/molecules26195934

[2] Lee YM. English Names for Korean Native Plants. Korea National Arboretum, Seoul, Korea: Korea Forest Service, 2015.

[3] Park J, Jeon YD, Kim HL, Kim DS, Han YH et al. Veratri Nigri Rhizoma et Radix (*Veratrum nigrum* L.) and its constituent jervine prevent adipogenesis via activation of the LKB1-AMPKα-ACC axis in vivo and in vitro. Evidence-Based Complementary and Alternative Medicine 2016; 2016: 8674397. https://doi.org/10.1155/2016/8674397

[4] Schep LJ, Schmierer DM, Fountain JS. *Veratrum* poisoning. Toxicological Reviews 2006; 25 (2): 73-78. https://doi.org/10.2165/00139709-200625020-00001

[5] Gao LJ, Zhang MZ, Li XY, Huang WK, Xu SF et al. Steroidal alkaloids isolated from *Veratrum grandiflorum* Loes. as novel smoothened inhibitors with anti-proliferation effects on DAOY medulloblastoma cells. Bioorganic and Medicinal Chemistry 2021; 39: 116166. https://doi.org/10.1016/j.bmc.2021.116166

[6] Li HJ, Jiang Y, Li P. Chemistry, bioactivity and geographical diversity of steroidal alkaloids from the Liliaceae family. Natural Product Reports 2006; 23 (5): 735-752. https://doi.org/10.1039/b609306j

[7] Kang CH, Han JH, Oh J, Kulkarni R, Zhou W. Steroidal alkaloids from *Veratrum nigrum* enhance glucose uptake in skeletal muscle cells. Journal of Natural Products 2015; 78 (4): 803-810. https://doi.org/10.1021/np501049g

[8] Yuan WJ, Zhu PY, Qiao M, Gao WF, Li GD. Two new steroidal alkaloids with cytotoxic activities from the roots of *Veratrum grandiflorum* Loes. Phytochemistry Letters 2021; 46: 56-60. https://doi.org/10.1016/j.phytol.2021.08.012

[9] Zhou CX, Liu JY, Ye WC, Liu CH, Tan RX. Neoverataline A and B, two antifungal alkaloids with a novel carbon skeleton from *Veratrum taliense*. Tetrahedron 2003; 59 (30): 5743-5747. https://doi.org/10.1016/S0040-4020(03)00882-2

[10] Cong Y, Wu Y, Shen S, Liu X, Guo J. A structure-activity relationship between the *Veratrum* alkaloids on the antihypertension and DNA damage activity in mice. Chemistry & Biodiversity 2020; 17 (2): e1900473. https://doi.org/10.1002/cbdv.201900473

[11] Xie TZ, Zhao YL, Wang H, Chen YC, Wei X et al. New steroidal alkaloids with anti-inflammatory and analgesic effects from *Veratrum grandiflorum*. Journal of Ethnopharmacology 2022; 293: 115290. https://doi.org/10.1016/j.jep.2022.115290

[12] Dumlu FA, Aydin T, Odabasoglu F, Berktas OA, Kutlu Z et al. Anti-inflammatory and antioxidant properties of jervine, a sterodial alkaloid from rhizomes of *Veratrum album*. Phytomedicine 2019; 55: 191-199. https://doi.org/10.1016/j.phymed.2018.06.035

[13] Xie TZ, Luo L, Zhao YL, Li H, Xiang ML et al. Steroidal alkaloids with a potent analgesic effect based on N-type calcium channel inhibition. Organic Letters 2022; 24 (2): 467-471. https://doi.org/10.1021/acs.orglett.1c02853

[14] Li Q, Zhao YL, Long CB, Zhu PF, Liu YP et al. Seven new veratramine-type alkaloids with potent analgesic effect from *Veratrum taliense*. Journal of Ethnopharmacology 2019; 244: 112137. https://doi.org/10.1016/j.jep.2019.112137

[15] Li W, Batu J, Zhang P, Wang S, Zhang X et al. Neoveratrol A-D: Four new arylbenzofurans from *Veratrum nigrum*. Phytochemistry Letters 2020; 40: 144-147. https://doi.org/10.1016/j.phytol.2020.09.010

[16] Zhao W, Tezuka Y, Kikuchi T, Chen J, Guo Y. Studies on the constitutents of *Veratrum* plants. II. Constituents of *Veratrum nigrum* L. var. *ussuriense*. (1). Structure and ^{1}H- and ^{13}C-nuclear magnetic resonance spectra of a new alkaloid, verussurinine, and related alkaloids. Chemical and Pharmaceutical Bulletin 1991; 39 (3): 549-554. https://doi.org/10.1248/cpb.39.549

[17] Khanfar MA, El Sayed KA. The *Veratrum* alkaloids jervine, veratramine, and their analogues as prostate cancer migration and proliferation inhibitors: biological evaluation and pharmacophore modeling. Medicinal Chemistry Research 2013; 22 (10): 4775-4786. https://doi.org/10.1007/s00044-013-0495-6

[18] El Sayed KA, McChesney JD, Halim AF, Zaghloul AM, Voehler M. Two steroidal alkaloids from *Veratrum viride*. Phytochemistry 1995; 38 (6): 1574-1550. https://doi.org/10.1016/0031-9422(94)00825-E

[19] Li YL, Zhang Y, Zhao PZ, Hu ZX, Gu YC et al. Two new steroidal alkaloids from the rhizomes of *Veratrum nigrum* L. and their anti-TYLCV activity. Fitoterapia 2020; 147; 104731. https://doi.org/10.1016/j.fitote.2020.104731

[20] Tang J, Li HL, Li YL, Zhang WD. Flavonoids from rhizomes of *Veratrum dahuricum*. Chemistry of Natural Compounds 2007; 43 (6): 696-697. https://doi.org/10.1007/s10600-007-0233-8

[21] Dai LM, Tang J, Li HL, Shen YH, Peng CY et al. A new stilbene glycoside from the *n*-butanol fraction of *Veratrum dahuricum*. Chemistry of Natural Compounds 2009; 45 (3): 325-329. https://doi.org/10.1007/s10600-009-9352-8

[22] Huang HQ, Li HL, Tang J, Lv YF, Zhang WD. A new aurone and other phenolic constituents from *Veratrum schindleri* Loes. f. Biochemical Systematics and Ecology 2008; 36 (7): 590-592. https://doi.org/10.1016/j.bse.2008.03.008

[23] Suh Y, Pak JH, Heo K, Paik WK, Chang K et al. Type specimens collected from Korea at the herbarium of the University of Tokyo. Seoul, Korea: Korea National Arboretum, 2015, 15: pp. 188-189.

[24] Lee SY, Choi SU, Lee JH, Lee DU, Lee KR. A new phenylpropane glycoside from the rhizome of *Sparganium stoloniferum*. Archives of Pharmacal Research 2010; 33 (4): 515-521. https://doi.org/10.1007/s12272-010-0404-1

[25] Teguo PW, Decendit A, Vercauteren J, Deffieux G, Merillon JM. *Trans*-resveratrol-3-*O*-β-glucoside (piceid) in cell suspension cultures of *Vitis vinifera*. Phytochemistry 1996; 42 (6): 1591-1593. https://doi.org/10.1016/0031-9422(96)00203-8

[26] Kanchanapoom T, Suga K, Kasai R, Yamasaki K, Kamel MS et al. Stilbene and 2-arylbenzofuran glucosides from the rhizomes of *Schoenocaulon officinale*. Chemical and Pharmaceutical Bulletin 2002; 50 (6): 863-865. https://doi.org/10.1248/cpb.50.863

[27] Kim HJ, Chang EJ, Bae SJ, Shim SM, Park HD et al. Cytotoxic and antimutagenic stilbenes from seeds of *Paeonia lactiflora*. Archives of Pharmacal Research 2002; 25 (3): 293-299. https://doi.org/10.1007/BF02976629

[28] Burns DC, Ellis DA, March RE. A predictive tool for assessing ^{13}C NMR chemical shifts of flavonoids. Magnetic Resonance in Chemistry 2007; 45 (10): 835-845. https://doi.org/10.1002/mrc.2054

[29] Wang Y, Shen JZ, Chan YW, Ho WS. Identification and growth inhibitory activity of the chemical constituents from *Imperata cylindrica* aerial part ethyl acetate extract. Molecules 2018; 23 (7): 1807. https://doi.org/10.3390/molecules23071807

[30] Tai BH, Cuong NM, Huong TT, Choi EM, Kim JA et al. Chrysoeriol isolated from the leaves of *Eurya ciliata* stimulates proliferation and differentiation of osteoblastic MC3T3-E1 cells. Journal of Asian Natural Products Research 2009; 11 (9-10): 817-823. https://doi.org/10.1080/10286020903117317

[31] Saeidnia S, Barari E, Shakeri A, Gohari AR. Isolation and identification of main compounds of *Lagochilus cabulicus*. Asian Journal of Chemistry 2013; 25 (3): 1509-1511. https://doi.org/10.14233/ajchem.2013.13117

[32] Lee JY, Cho YR, Park JH, Ahn EK, Jeong W et al. Anti-melanogenic and anti-oxidant activities of ethanol extract of *Kummerowia striata*: *Kummerowia striata* regulate anti-melanogenic activity through down-regulation of TRP-1, TRP-2 and MITF expression. Toxicology Reports 2018; 3 (6): 10-17. https://doi.org/10.1016/j.toxrep.2018.11.005

[33] Kraunsoe JAE, Claridge TDW, Lowe G. Inhibition of human leukocyte and porcine pancreatic elastase by homologues of bovine pancreatic trypsin inhibitor. Biochemistry 1996; 35 (28): 9090-9096. https://doi.org/10.1021/bi953013b

[34] Ko RK, Kim GO, Hyun CG, Jung DS, Lee NH. Compounds with tyrosinase inhibition, elastase inhibition and DPPH radical scavenging activities from the branches of *Distylium racemosum* Sieb. et Zucc. Phytotherapy Research 2011; 25 (10): 1451-1456. https://doi.org/10.1002/ptr.3439

[35] Markham KR, Ternai B, Stanley R, Geiger H, Mabry TJ. Carbon-^{13}NMR studies of flavonoids-III: naturally occurring flavonoid glycosides and their acylated derivatives. Tetrahedron 1978; 34 (9): 1389-1397. https://doi.org/10.1016/0040-4020(78)88336-7

[36] Zolghadri S, Bahrami A, Hassan Khan MT, Munoz-Munoz J, Garcia-Molina F et al. A comprehensive review on tyrosinase inhibitors. Journal of Enzyme Inhibition and Medicinal Chemistry 2019; 34 (1): 279-309. https://doi.org/10.1080/14756366.2018.1545767

[37] Kim C, Park J, Lee H, Hwang DY, Park SH et al. Evaluation of the EtOAc extract of lemongrass (*Cymbopogon citratus*) as a potential skincare cosmetic material for acne vulgaris. Journal of Microbiology and Biotechnology 2022; 32 (5): 594-601. https://doi.org/10.4014/jmb.2201.01037

[38] Peng LH, Liu S, Xu SY, Chen L, Shan YH et al. Inhibitory effects of salidroside and paeonol on tyrosinase activity and melanin synthesis in mouse B16F10 melanoma cells and ultraviolet B-induced pigmentation in guinea pig skin. Phytomedicine 2013; 20 (12): 1082-1087. https://doi.org/10.1016/j.phymed.2013.04.015

Supporting Information

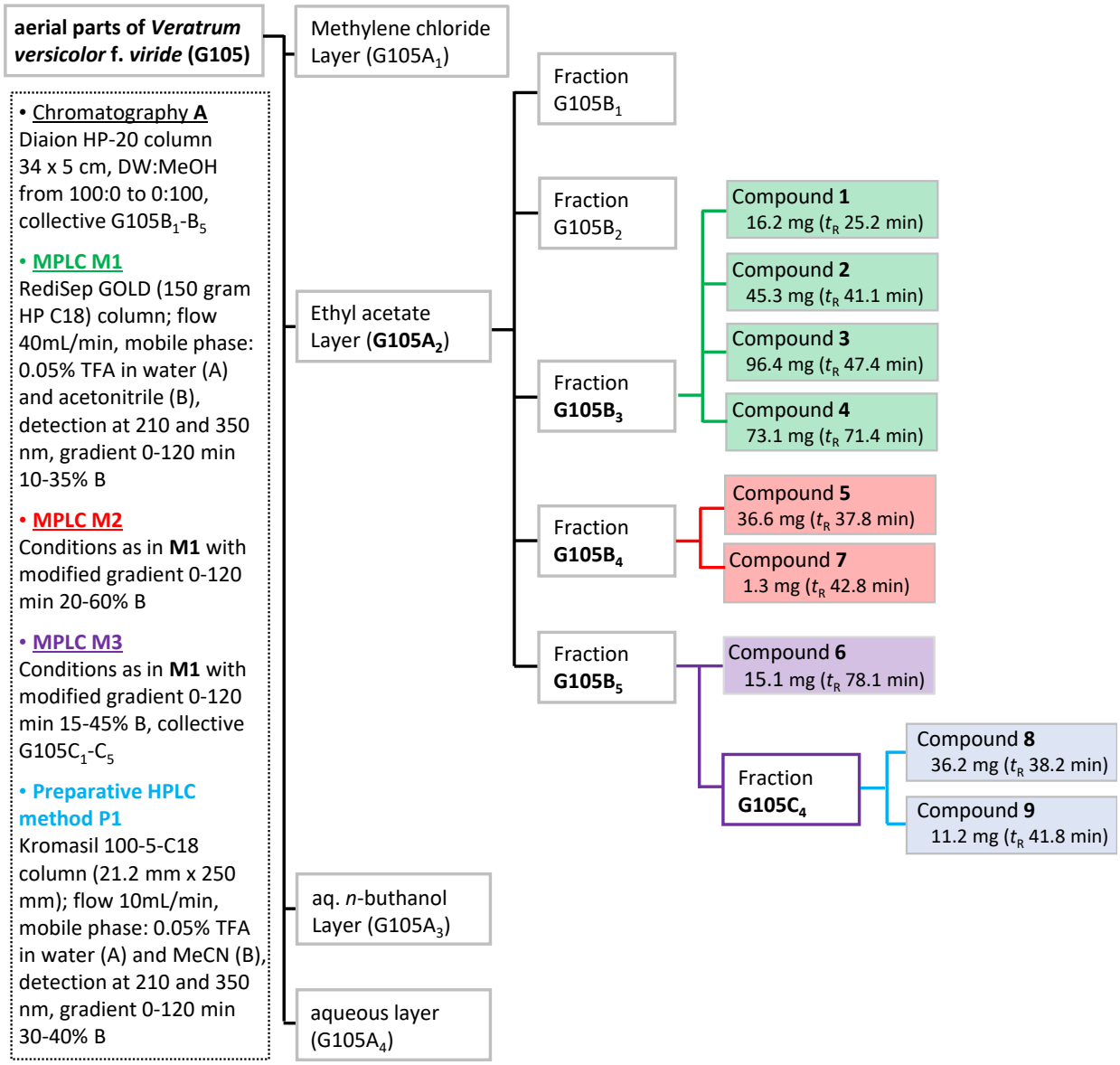

Figure S1. The isolation scheme of compounds **1**–**9**.

1. Apparatus and chromatographic conditions

HPLC analysis was performed on a Waters alliance e2695 (Waters Co., Milford, MA, USA) system composed of a 2998 PDA detector and column heater/cooler with a passive preheater. The separation was achieved using a YMC-Triart C18 column (250 × 4.6 mm I.D., 5 µm particle size) (YMC Co., Ltd., Japan). The mobile phase consisted of water–TFA (99.95:0.05; v/v) (solvent A) and acetonitrile (solvent B). The elution was performed using the following gradient: initial 90:10 (A:B v/v); 60 min 60:40 (A:B v/v). The mobile phase was prepared daily, filtered through a 0.45-mm, WTP 0.5-mm membrane (Whatmann, Maidstone, UK), sonicated before use and delivered at a flow rate of 1.0 mL/min. The injection volume was 10 µL and the column temperature was at 25 °C. All the operations, the acquiring and analysis of data were controlled by Empower 3 Software (Waters Co., Milford, MA, USA).

Table S1. Inhibitory activity (melanin contents) of compounds isolated from *V. versicolor* f. *viride* on melanogenesis in B16 mouse melanoma cells.

Compound	Melanin contents (%)			
	25 μM	50 μM	100 μM	400 μM
1	91.30 ± 4.81[a]	74.78 ± 0.69	64.01 ± 1.45	
2	136.33 ± 3.36	132.31 ± 6.52	116.14 ± 6.39	
3	117.63 ± 3.73	108.76 ± 1.96	29.56 ± 2.21	
4	82.28 ± 1.18	27.29 ± 5.83	17.30 ± 0.01	
5	17.98 ± 0.76	16.41 ± 1.65	8.99 ± 0.73	
6	83.60 ± 3.01	63.16 ± 2.11	16.24 ± 1.52	
7	65.25 ± 1.18	65.37 ± 1.41	56.39 ± 0.89	
8	37.02 ± 4.57	27.32 ± 0.80	23.36 ± 2.19	
Arbutin[b]				30.71 ± 3.34

[a]All compounds were examined in a set of experiments three times.
[b]Positive control.

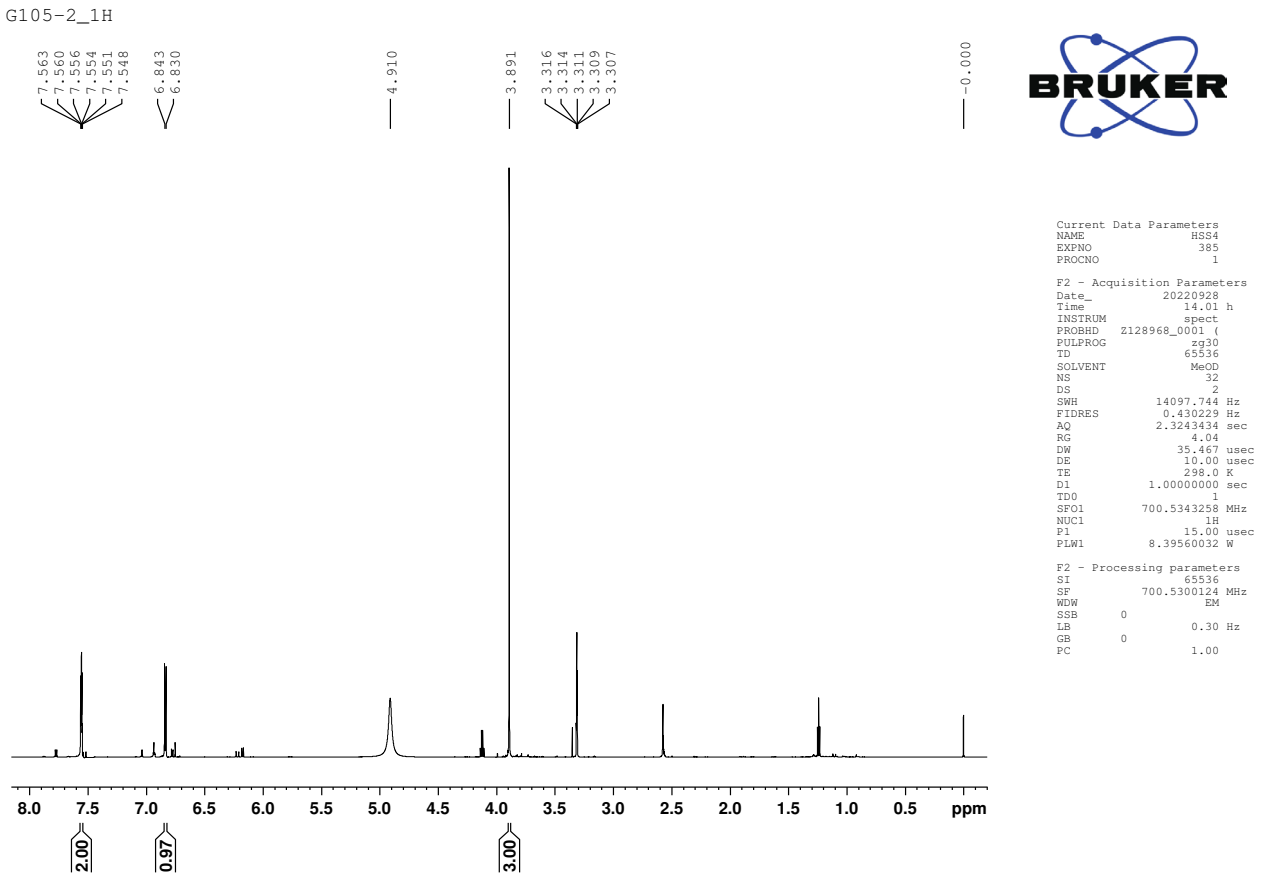

Figure S2. ^{1}H NMR spectrum (CD_3OD, 700 MHz) of compound **1**.

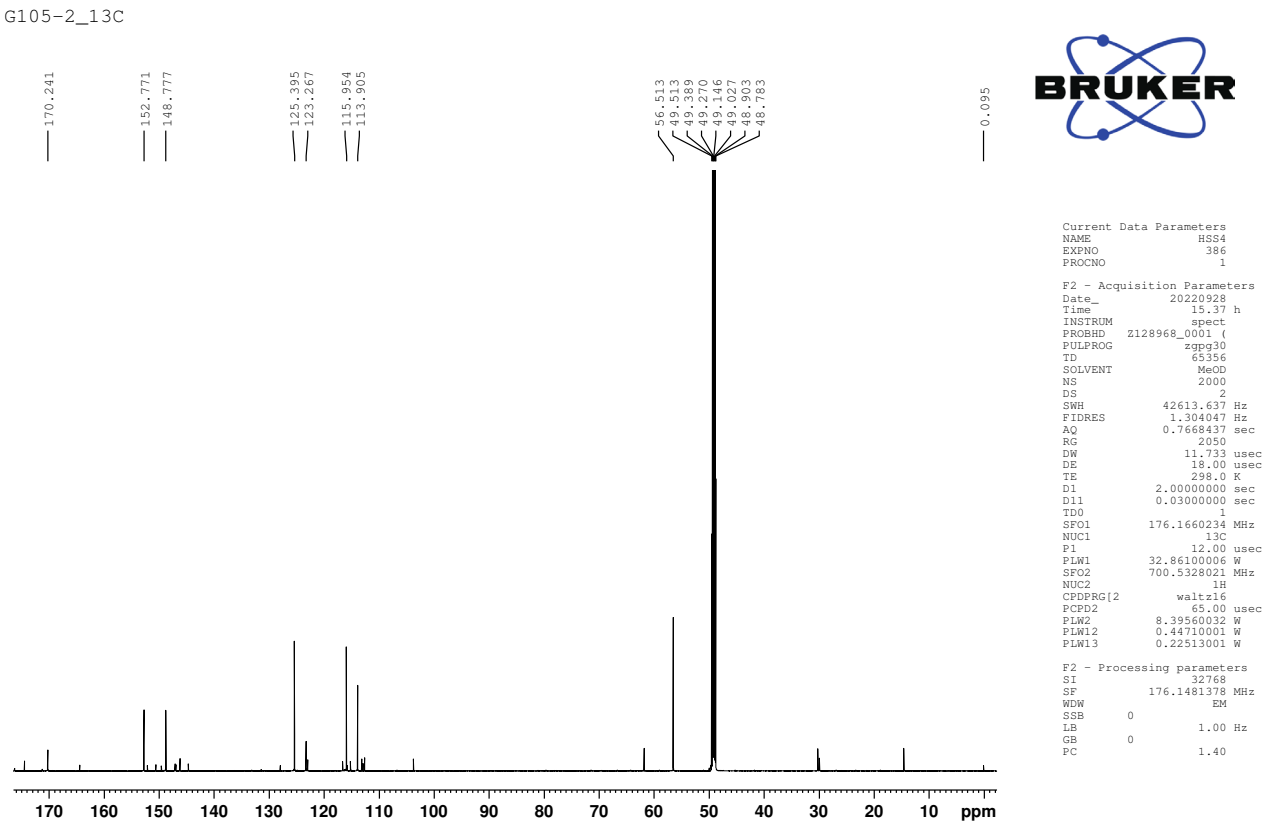

Figure S3. ^{13}C NMR spectrum (CD_3OD, 175 MHz) of compound **1**.

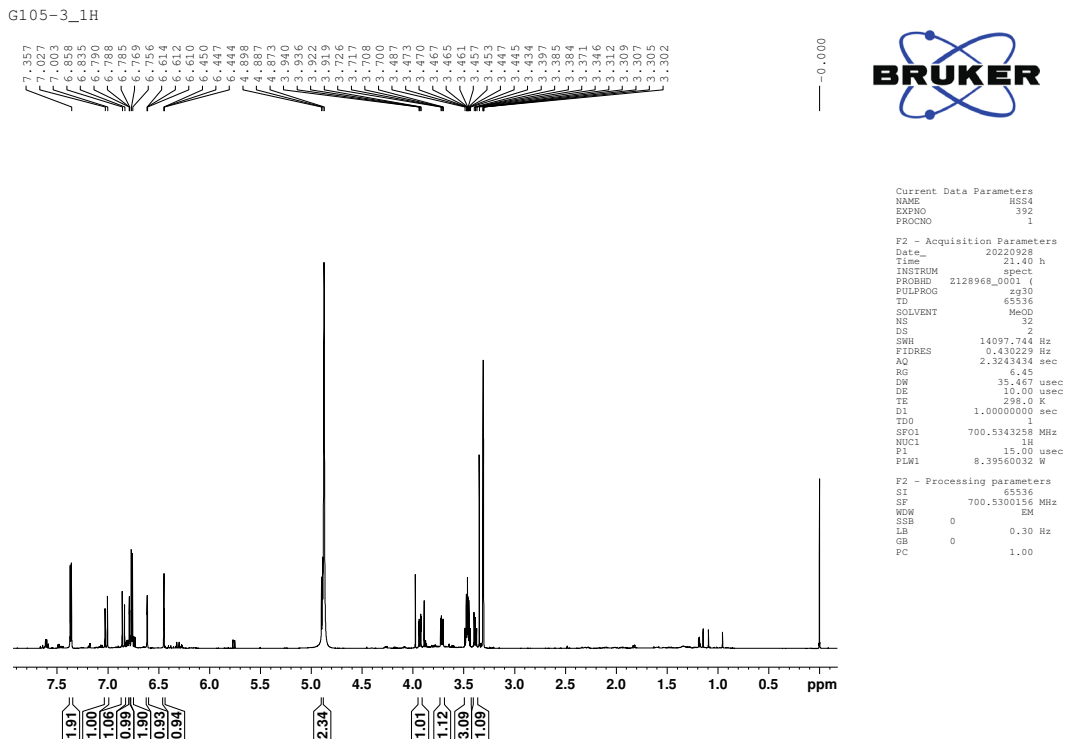

Figure S4. ^{1}H NMR spectrum (CD_3OD, 700 MHz) of compound **2**.

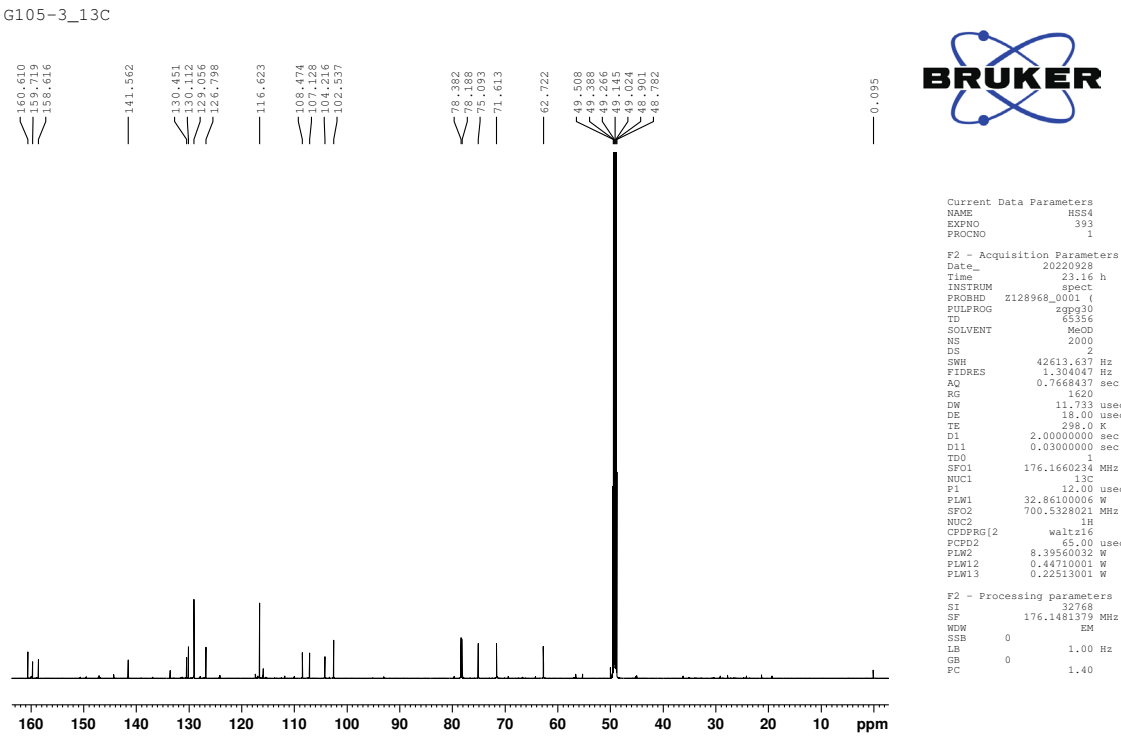

Figure S5. ^{13}C NMR spectrum (CD_3OD, 175 MHz) of compound **2**.

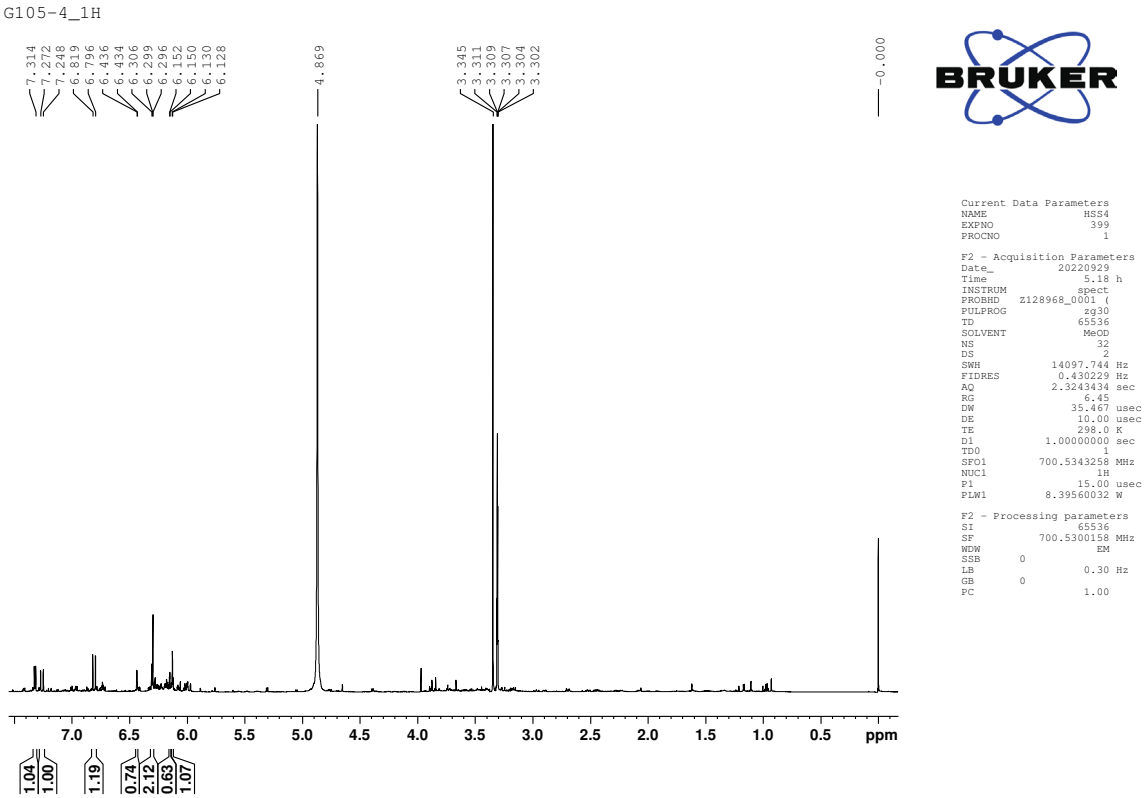

Figure S6. ^{1}H NMR spectrum (CD_3OD, 700 MHz) of compound **3**.

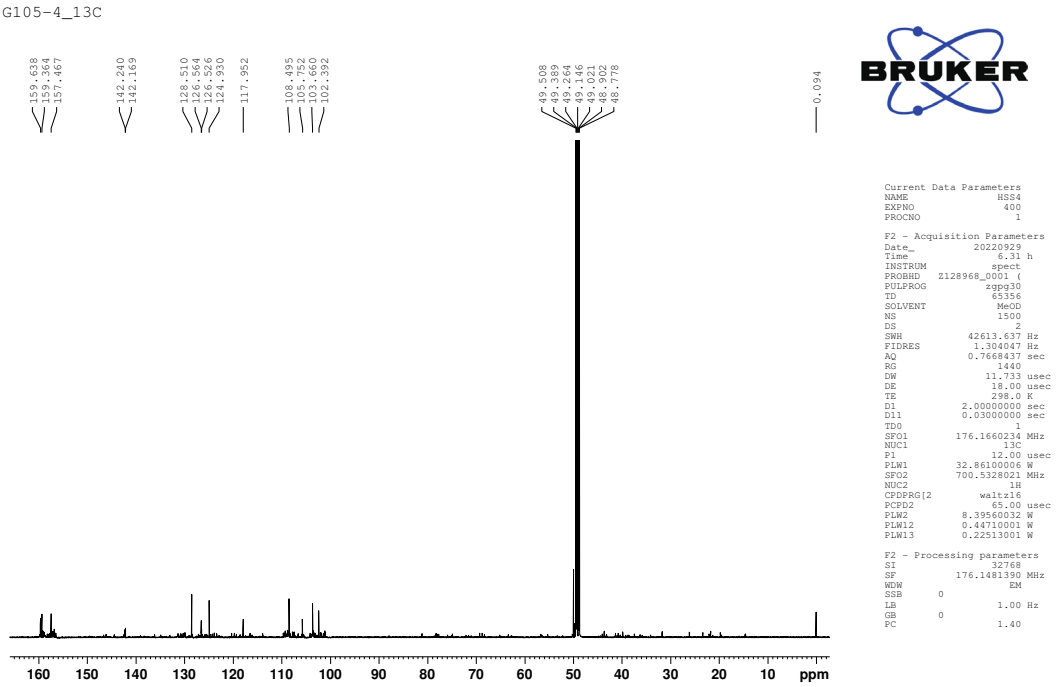

Figure S7. ^{13}C NMR spectrum (CD_3OD, 175 MHz) of compound **3**.

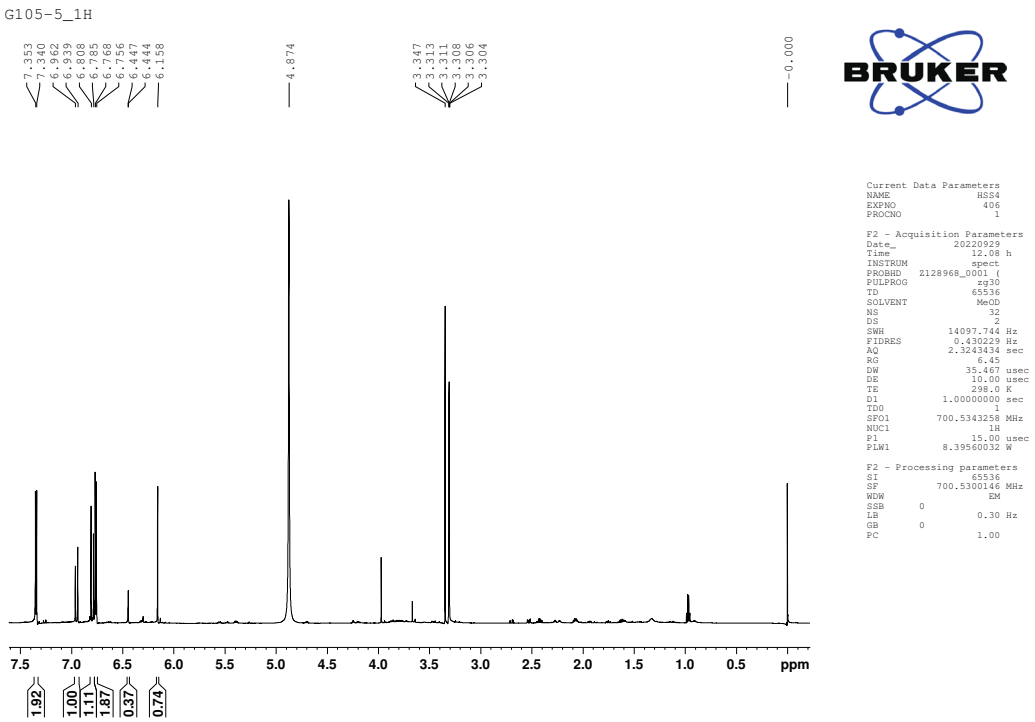

Figure S8. ^{1}H NMR spectrum (CD_3OD, 700 MHz) of compound **4**.

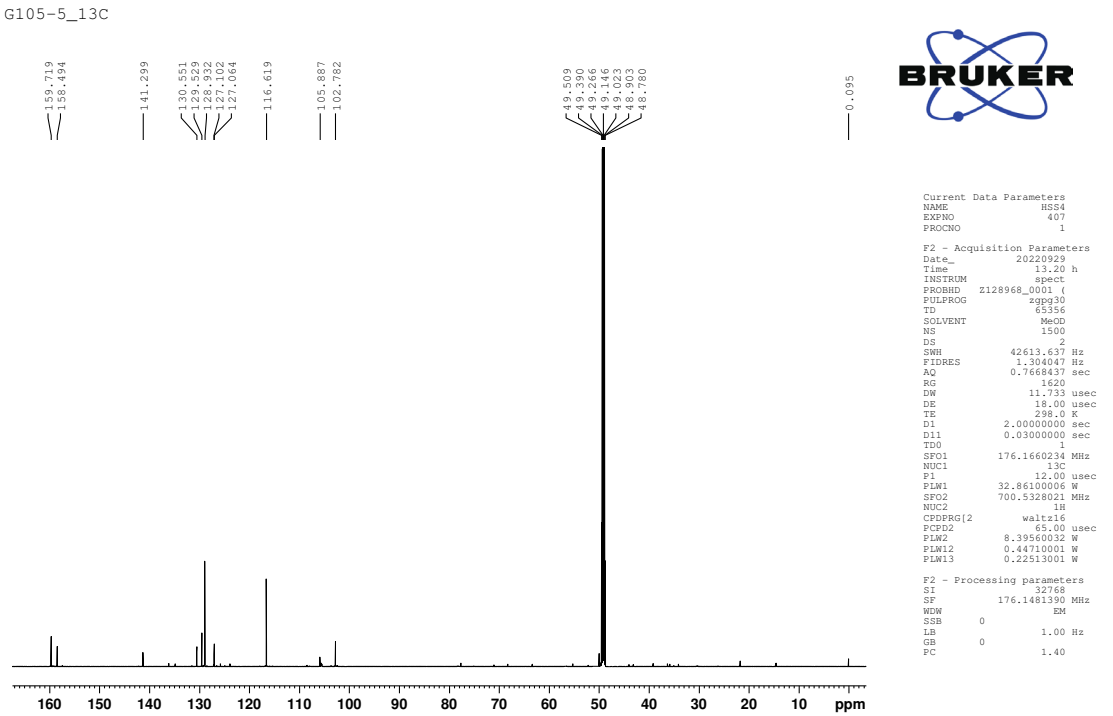

Figure S9. ^{13}C NMR spectrum (CD_3OD, 175 MHz) of compound **4**.

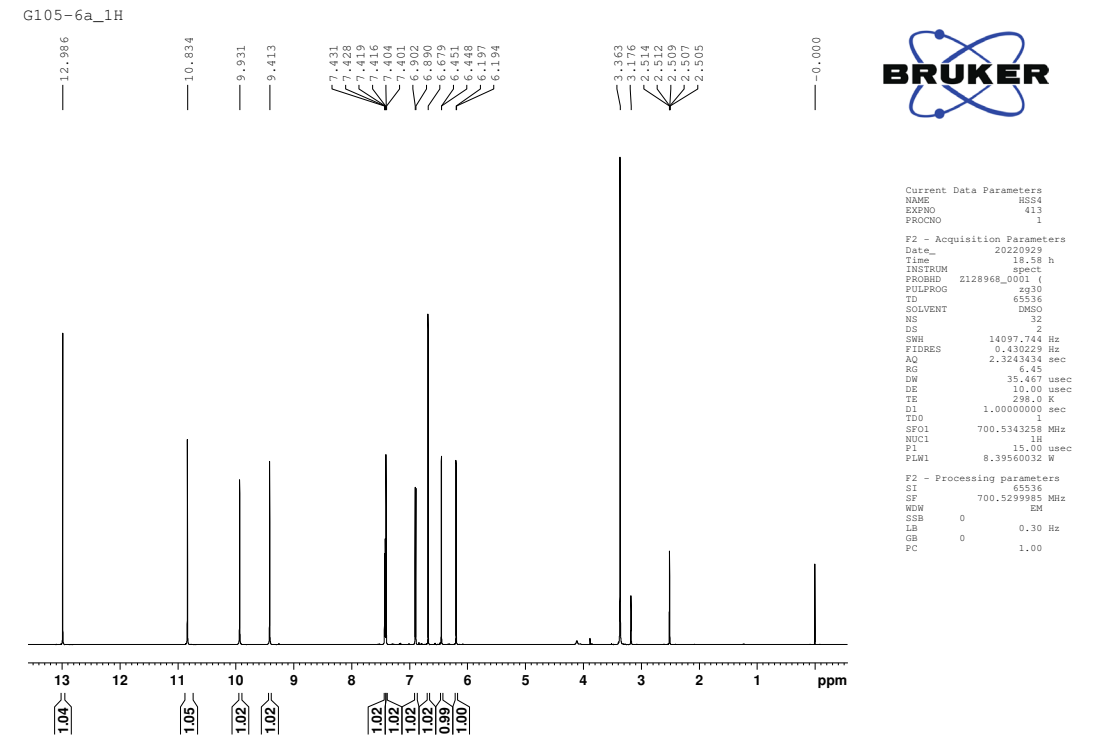

Figure S10. ^{1}H NMR spectrum (DMSO-d_6, 700 MHz) of compound **5**.

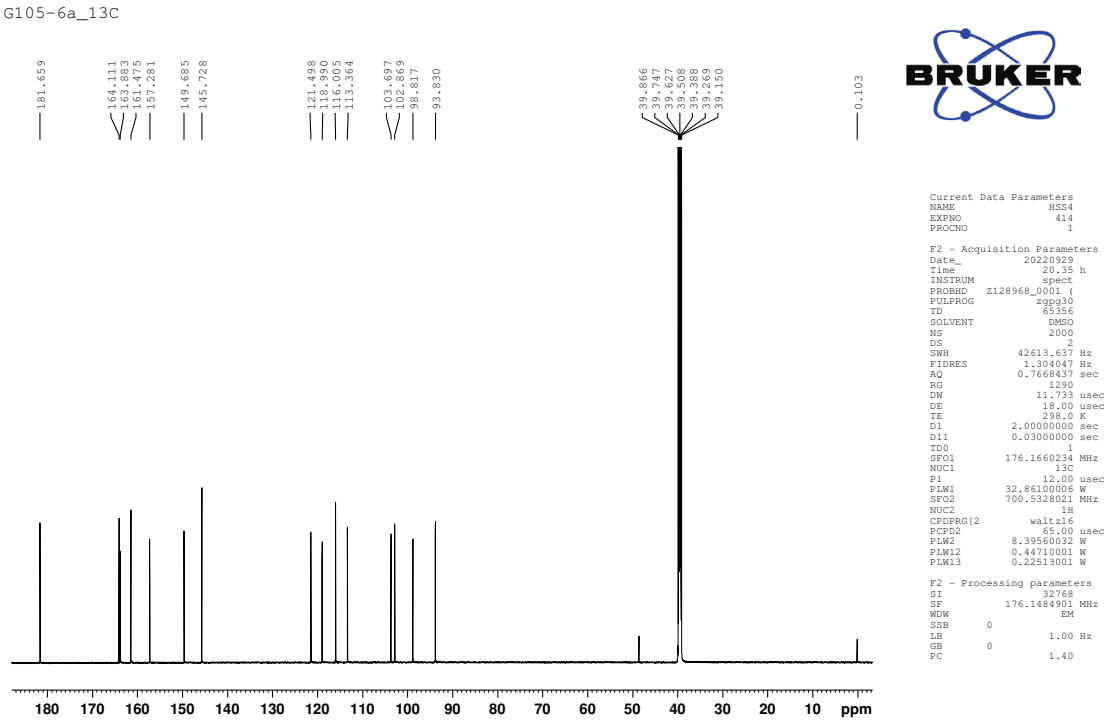

Figure S11. ^{13}C NMR spectrum (DMSO-d_6, 175 MHz) of compound **5**.

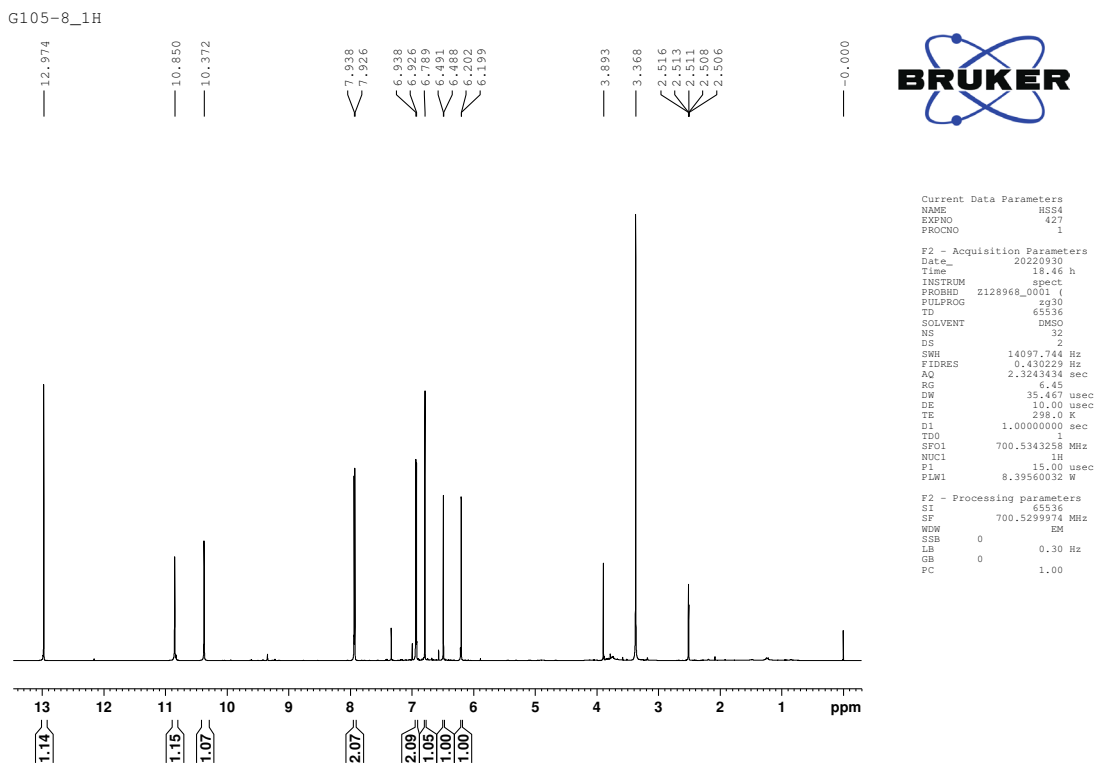

Figure S12. ^{1}H NMR spectrum (DMSO-d_6, 700 MHz) of compound **6**.

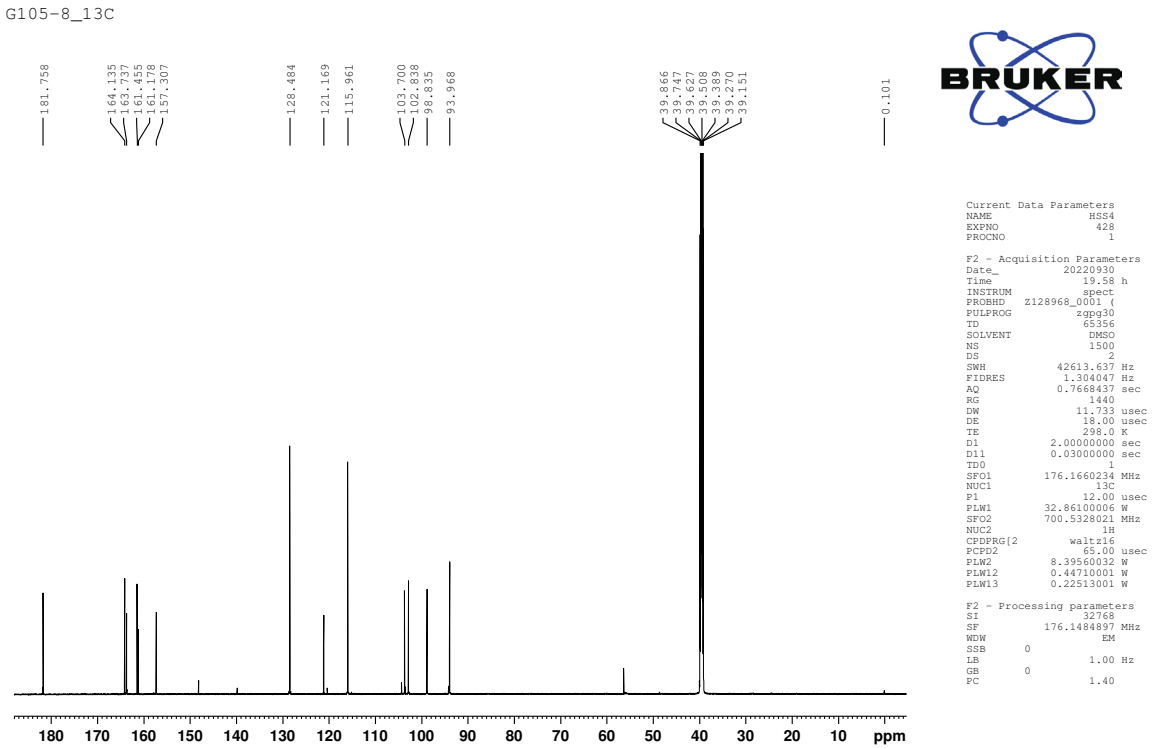

Figure S13. ^{13}C NMR spectrum (DMSO-d_6, 175 MHz) of compound **6**.

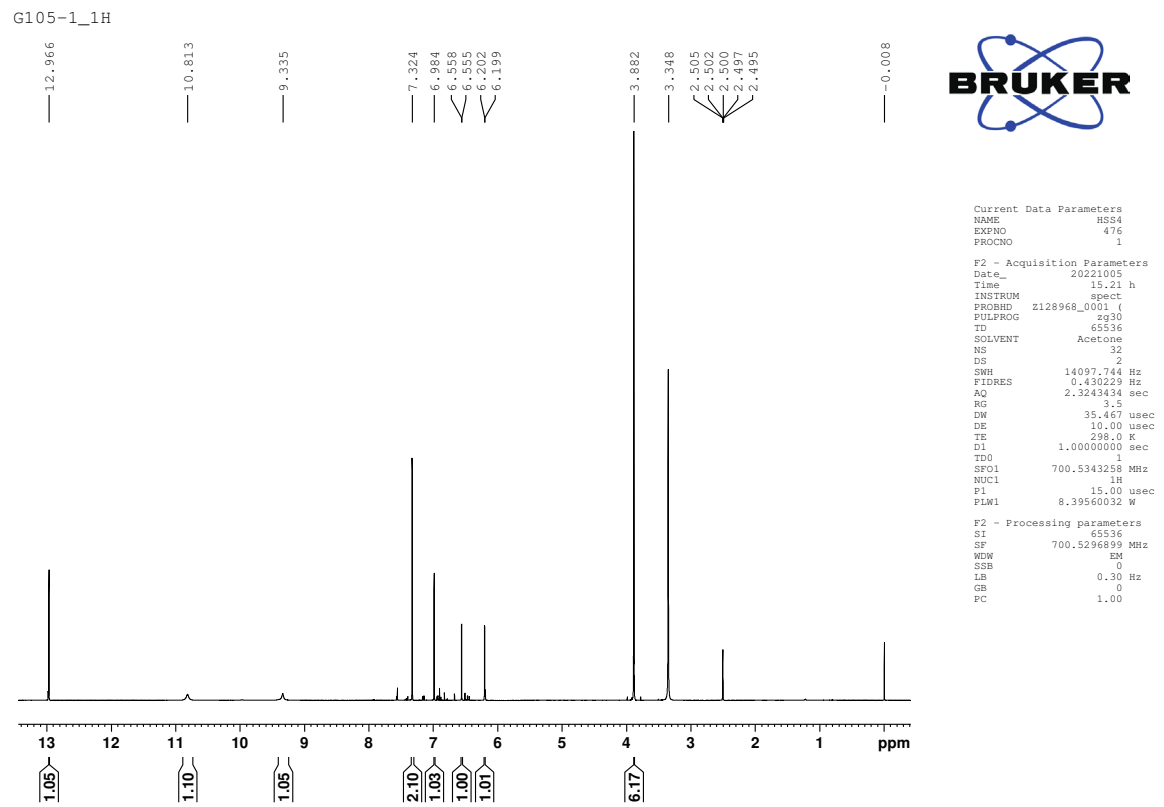

Figure S14. ^{1}H NMR spectrum (DMSO-d_6, 700 MHz) of compound **7**.

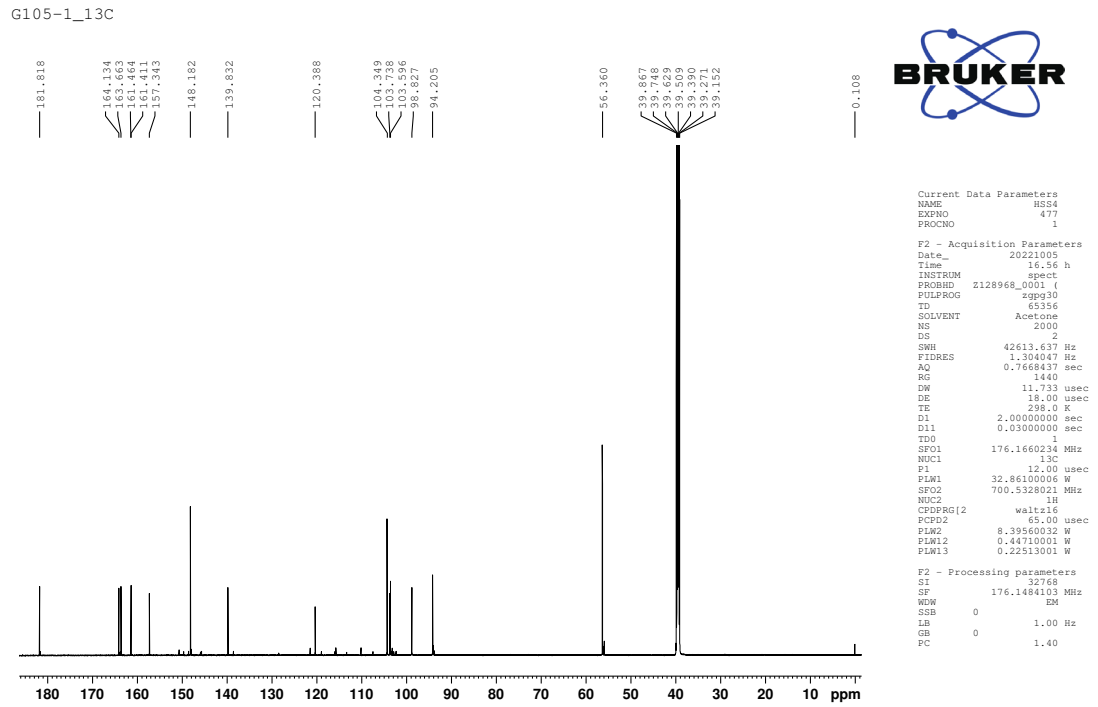

Figure S15. ^{13}C NMR spectrum (DMSO-d_6, 175 MHz) of compound **7**.

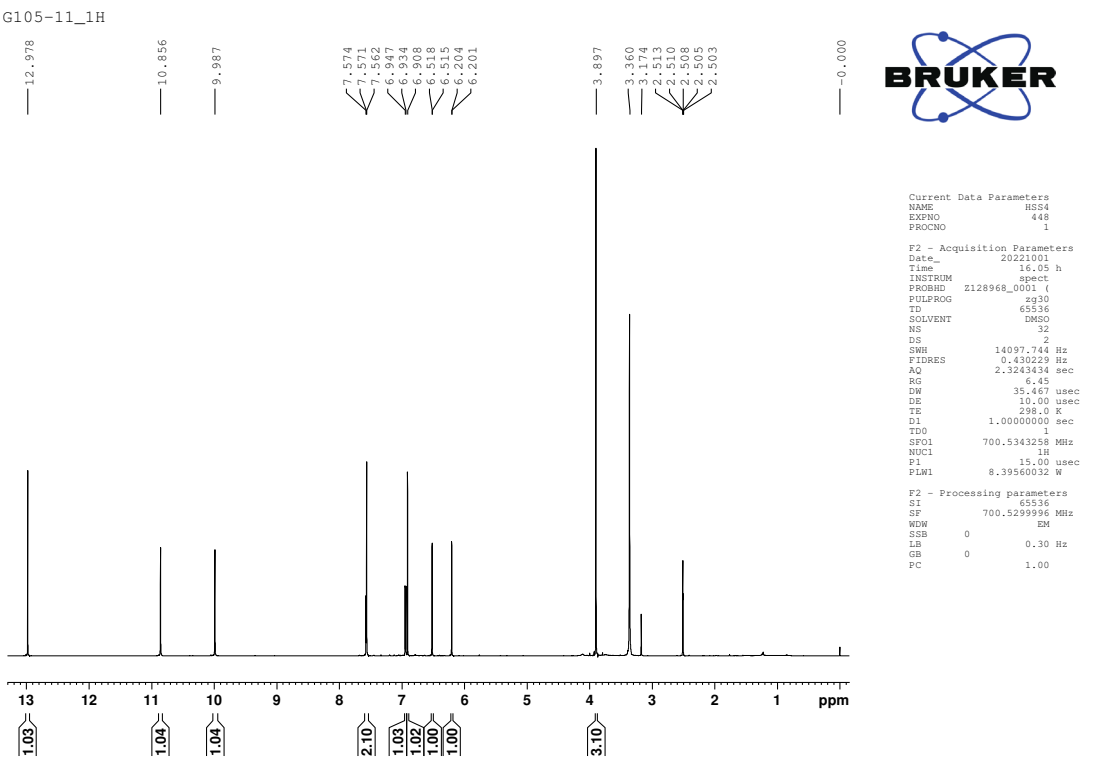

Figure S16. ^{1}H NMR spectrum (DMSO-d_6, 700 MHz) of compound **8**.

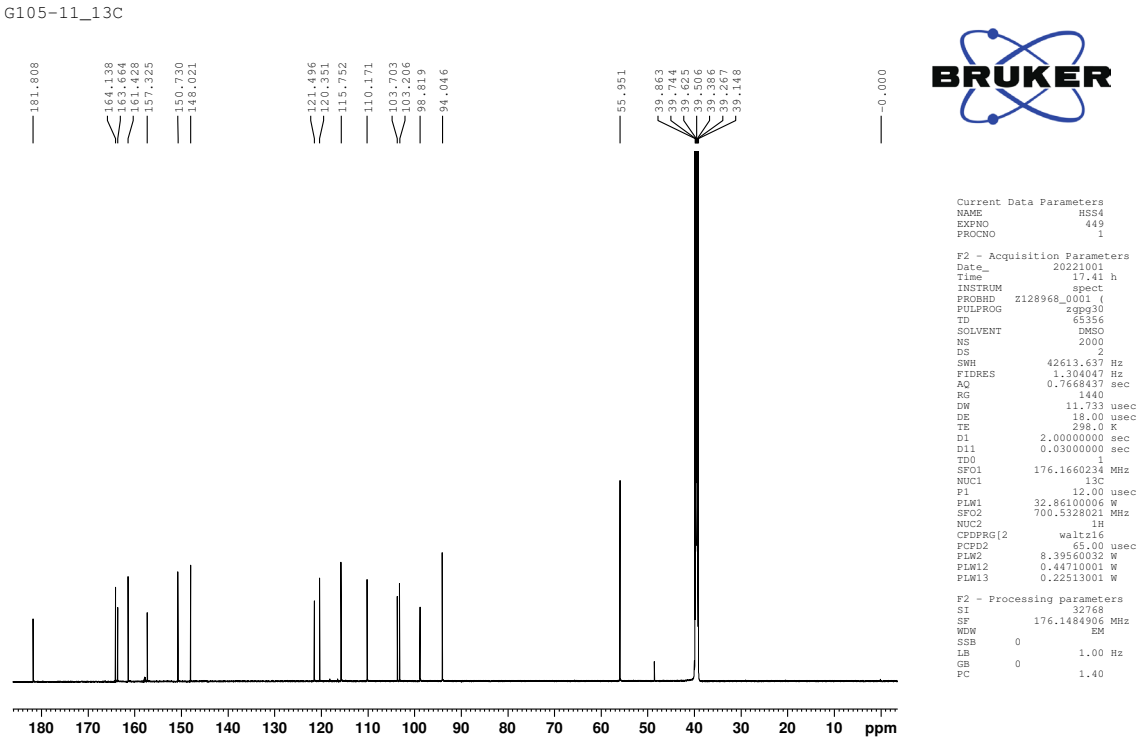

Figure S17. ^{13}C NMR spectrum (DMSO-d_6, 175 MHz) of compound **8**.

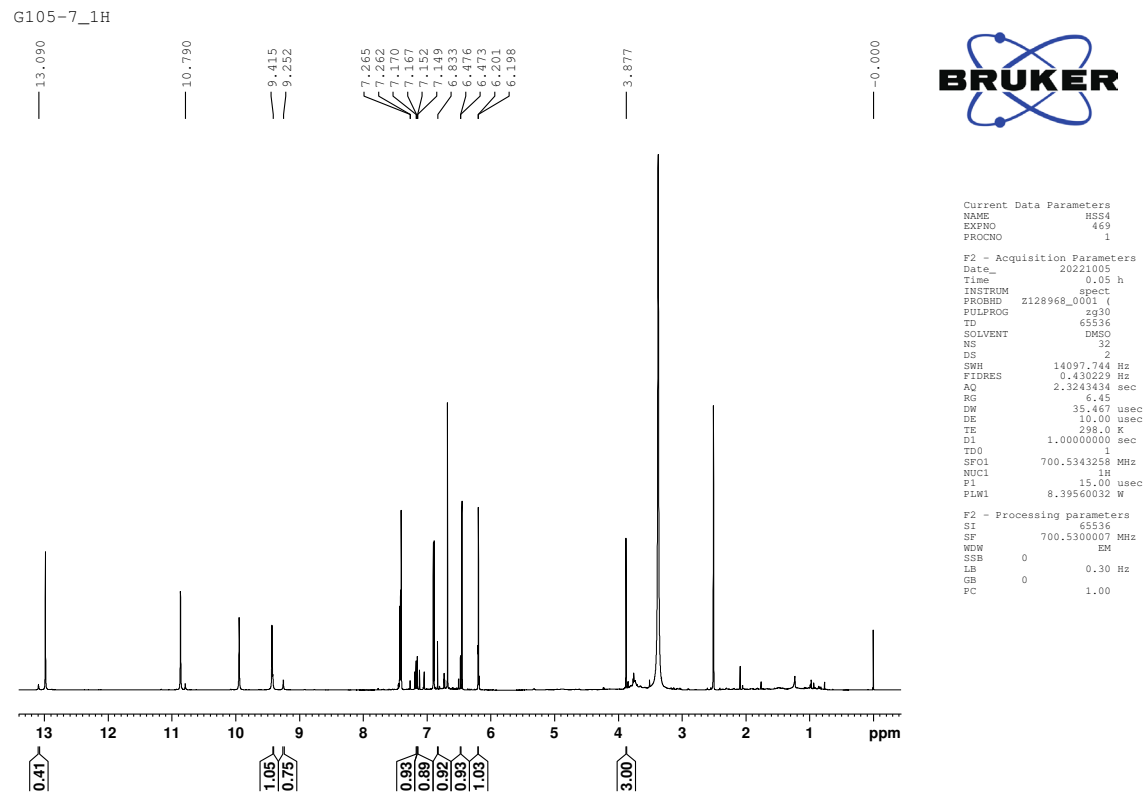

Figure S18. ^{1}H NMR spectrum (DMSO-d_6, 700 MHz) of compound **9**.

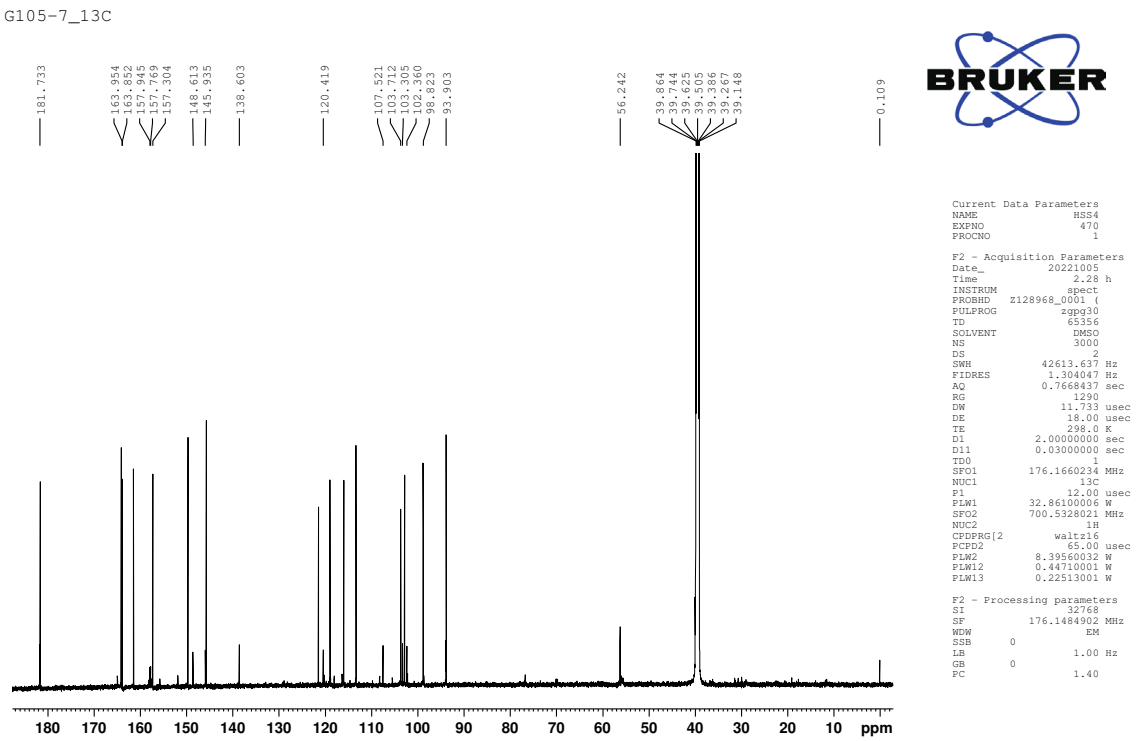

Figure S19. ^{13}C NMR spectrum (DMSO-d_6, 175 MHz) of compound **9**.